

Chapter 7

\hbar corrections

7.1 \hbar corrections to the Gutzwiller trace formula

The Gutzwiller trace formula (4.21) is the most compact formulation of the semiclassical quantization of multidimensional systems. In recent years it has been demonstrated[35] on many classically chaotic systems that it is indeed a very good approximation.

As mentioned the starting point of the Gutzwiller derivation of the trace formula can be taken in the Feynman path integral form[27, 50] of the propagator. But, calculations with path integrals are difficult in general. It is often easier to find the numerical solution of the underlying Schrödinger equation. The most convenient asymptotic method to evaluate the path integral is the saddle point approximation. The leading Gaussian approximation is easy to perform and gives very good results, as we saw in the two previous sections.

There are many attempts to improve the semiclassical approximation within the framework of the Gaussian approximation in order to get accurate energies and resonances. But the Gaussian approximation has its inherent limitation and one should go beyond it to improve the accuracy. Recently, Gaspard and Alonso [33] computed corrections of the Gutzwiller trace formula and showed that the resonances of the two and three disk scattering systems[32, 61] can be improved considerably. They have used the usual Feynman graph technique of the perturbation theory and computed large number of graphs to get the corrections. In general the conventional graph calculus is very cumbersome. In this chapter we shall describe an alternative approach to the calculation of \hbar corrections, using ordinary differential equations.

The basic idea is the following. Suppose you have a time independant bound system and are looking for the energy eigenvalues of the Hamilton operator. An eigenfunction ψ_n , fulfills the time independant Schrödinger equation

$$\hat{H}\psi_n = E_n\psi_n. \quad (7.1)$$

Now if you consider a periodic orbit of the corresponding classical system, then

you can expand the potential in the Hamiltonian around this orbit and try to solve the Schrödinger problem with appropriate boundary conditions in the neighbourhood of this orbit. This will in general give a complete eigenspectrum with corresponding eigenfunctions. However, since the local problem contains the full problem as a special case, the original spectrum will be contained in the local spectrum. If you now follow the same procedure for all the periodic orbits in the system, and if the set of periodic orbits are sufficiently proliferating then the union of restrictions prescribed by all the periodic orbits will finally lead to the spectrum we were originally looking for. Now the \hbar correction scheme enters in the solution of the local Schrödinger problem. If we make the usual ansatz that the local wave function is given by

$$\psi_p = \varphi_p e^{iS_p/\hbar}, \quad (7.2)$$

then by inserting this expression into the local Schrödinger equation and expanding in orders of \hbar , we end up with the Hamilton-Jacobi equation for the (local) action S_p and with an evolution equation for the amplitude φ . In this last equation one usually neglects the \hbar^2 term and is then led to the classical continuity equation for the amplitude, which gives the usual semiclassical result as we saw in section 4.1. Here we instead expand the amplitude in a perturbation series in \hbar , and keep the \hbar^2 term in the equation for the purpose of connecting different orders in \hbar in the expansion. This results in an iterative scheme where the coefficients in the \hbar expansion of the amplitude can be determined successively. Finally the \hbar corrected amplitude function can then be connected to the spectral determinants of the local problem, and by multiplying these together, we finally end up with an \hbar corrected spectral determinant for the full problem.

The above considerations are of course in no sense rigorous but they give the main idea of the strategy we are going to follow in this chapter. It should be emphasised that the theory sketched in the following sections is *still not in complete mathematical rigour*. We take this theory as *the starting point*, and concentrate in this thesis on applications of the theory to billiard systems.

The strategy of this chapter is therefore the following: first we describe the method developed in [55] and obtain differential equations for computing \hbar corrections to the Gutzwiller trace formula. We then specialize to billiard systems and develop an algorithm to compute the corrections which using geometrical information about periodic orbits, such as their lengths, stabilities, bouncing angles etc. Finally we carry out several numerical computations on the two- and three-disk scattering systems and compare the results to the exact quantum results and to the work by Gaspard et al. [33] to show that our theory gives equivalent results.

7.2 Path integrals and partial differential equations

In this section we show how the path integral expression for the propagator can be connected to a set of partial differential equations in the case where

one uses the saddlepoint approximation to restrict the path integral to tubes around classical paths, or paths that has a minimal action.

The path integral representation of the propagator is

$$G(q, q', t) = \int \mathcal{D}q'' e^{\frac{i}{\hbar}S(q, q', t|q'')}, \quad (7.3)$$

where $\int \mathcal{D}q''$ represents the functional integral measure for all the paths connecting q with q' in time t , and $S(q, q', t|q'')$ is the classical action between q and q' computed along a given path q'' . We are interested in the path integral expression for the trace which reads

$$\text{Tr}G(t) = \int dq G(q, q, t) = \int \mathcal{D}q'' e^{\frac{i}{\hbar}S(t|q'')}, \quad (7.4)$$

where $\int \mathcal{D}q''$ now represents the functional integration for closed paths. In the saddle point approximation the leading contribution to the path integral is coming from the neighbourhood of paths for which the classical action is stationary. This condition singles out the classical periodic trajectories from the infinite variety of possible paths;

$$\text{Tr}G(t) = \sum_p \int \mathcal{D}q_p \exp\left(\frac{i}{\hbar}S_p(q_p, t)\right), \quad (7.5)$$

where \sum_p denotes the summation for the classical primitive periodic orbits and $\int \mathcal{D}q_p$ denotes a functional integral in the neighborhood of periodic orbits, where we Taylor expand the classical action around the periodic orbit $x_p(t)$

$$S_p(x, t) = \sum_{\mathbf{n}}^{\infty} s_{\mathbf{n}}(t)(x - x_p(t))^{\mathbf{n}} / \mathbf{n}!. \quad (7.6)$$

The symbol $\mathbf{n} = (n_1, n_2, \dots, n_d)$ denotes the multi index in d dimensions, $\mathbf{n}! = \prod_{i=1}^d n_i!$ the multi factorial and $(q_p - x_p(t))^{\mathbf{n}} = \prod_{i=1}^d (q_{p,i} - x_{p,i}(t))^{n_i}$, respectively.

Since the saddle points are taken in the configuration space, only spatially distinct periodic orbits, the so called primitive periodic orbits, appear in the summation. If we continue the standard textbook calculation scheme, we should truncate the Taylor expansion in the exponent at the quadratic order term while treating the higher order terms as corrections. Then we can compute the path integrals with the help of Gaussian integrals. In this way one can derive Gutzwiller's trace formula. Corrections to the Gaussian approximation can be found by expanding the action to higher orders, expanding the exponential and performing the Gaussian cumulant integrals.

Here we do not follow the textbook approach. Instead we observe that the terms in (7.5) are similar to the original path integral expression of the

trace (7.4). The only difference is that each term has to be computed in the neighborhood of a periodic orbit and that the classical actions are given in power series form.

We now consider the *local* Schrödinger equation,

$$\hat{H}_p \psi_p(x, t) = i\hbar \frac{\partial \psi_p(x, t)}{\partial t} \quad (7.7)$$

which leads to the *local* path sum

$$\int \mathcal{D}q_p e^{i/\hbar \sum_{\mathbf{n}} S_{\mathbf{n}}(x_p(t), t) q_p^{\mathbf{n}} / \mathbf{n}!} = \text{Tr} G_p(q_p, q_p', t). \quad (7.8)$$

The saddle point expansion of the full trace in terms of local traces then becomes

$$\text{Tr} G(x, x', t) = \text{Tr} G_W(x, x', t) + \sum_p \text{Tr} G_p(q_p, q_p', t), \quad (7.9)$$

where $G_W(x, x', t)$ denotes formally the Green function expanded around zero length (non moving) periodic orbits, known as the Weyl term[6]. Each Green function can be separately Fourier transformed and we get in the energy domain:

$$\text{Tr} G(x, x', E) = g_0(E) + \sum_p \text{Tr} G_p(q_p, q_p', E). \quad (7.10)$$

Notice, that in contrast to the derivation of section 4.1 we do not need here to take further saddle points in time, since we are dealing with exact time and energy domain Green functions.

The local spectral determinant $\Delta_p(E)$ for the local operators is defined as

$$\text{Tr} G_p(q_p, q_p', E) = \frac{d}{dE} \log \Delta_p(E). \quad (7.11)$$

Using (7.10) we can express the full spectral determinant as a product over the sub-determinants

$$\Delta(E) = e^{W(E)} \prod_p \Delta_p(E), \quad (7.12)$$

where $W(E) = \int^E g_0(E') dE'$ is the term coming from the Weyl expansion.

In general, there are many different types of closed periodic orbits which can contribute to the product (7.12). The spectral determinant of the zero length orbits gives a smooth contribution, which is the counterpart of the Weyl or Thomas-Fermi terms. From now on we neglect these terms since they do not change the location of the zeroes of the spectral determinant. Also, the periodic orbits in the complexified phase space of the Hamiltonian system can contribute[8], as well as the diffraction cycles introduced in section 6.1. In the following we concentrate only on the usual classical periodic orbits.

We should mention that here we do not investigate the general validity of the saddle point approximation. However, it is important to note that the power series expansion of the action is an asymptotic expansion, where contributions from different orbits overlap and this causes some overcounting in the formula (7.5). Therefore in computations the number of periodic orbits included in the sum should depend on the order of truncation of the power series. In the semiclassical or Gaussian approximation the criterion proposed by Berry and Keating [7] can be used. We hope, that a similar condition can be derived for the situation discussed here.

Local spectra of the Schrödinger equation

To compute the local spectral determinants $\Delta_p(E)$ we have to solve the local Schrödinger problem (7.7) in the neighborhood of a classical periodic orbit, and all variables should be indexed with a p . For simplicity we shall drop this index in the rest of this section.

The local Schrödinger equation

$$i\hbar\partial_t\psi = -\frac{\hbar^2}{2m}\Delta\psi + U\psi \quad (7.13)$$

can be constructed by expanding the Hamilton operator in the neighbourhood of the periodic orbit and imposing appropriate boundary conditions in the direction orthogonal to the velocity direction of the orbit. The boundary conditions are

$$\max_{|\vec{\mu}|=R}|A(s, \vec{\mu})| \rightarrow 0, \quad \text{for } R \rightarrow \infty \quad (7.14)$$

$$A(s+L, \vec{\mu}) = e^{i\kappa} A(s, \vec{\mu}) \quad (7.15)$$

where A is the amplitude of the wave function, s measures the length along the periodic orbit and $\vec{\mu}$ is a small vector orthogonal to the direction of the flow. With the conditions (7.15) the local Schrödinger equation (7.7) becomes a precisely formulated boundary value problem. This idea is described in detail and with all the mathematical rigour in [5].

The equation is most conveniently solved by rewriting it with the usual ansatz

$$\psi = \varphi e^{iS/\hbar}, \quad (7.16)$$

where we have not yet imposed any restrictions on the functions $\varphi(x, t)$ and $S(x, t)$. Inserting these equations into the Schrödinger equation (7.13) yields

$$\begin{aligned} -\varphi\partial_t S + i\hbar\partial_t\varphi &= -\frac{\hbar^2}{2}(\Delta\varphi + 2i/\hbar\nabla\varphi\nabla S \\ &\quad + i/\hbar\varphi\Delta S - 1/\hbar^2\varphi(\nabla S)^2) + U\varphi. \end{aligned} \quad (7.17)$$

Here we have many possibilities to group the terms since we have not made any restriction for S and φ yet. Our main concern is to separate the classical and the quantum time evolution. Therefore, we require the phase to fulfill the Hamilton-Jacobi equation

$$\partial_t S + \frac{1}{2}(\nabla S)^2 + U = 0. \quad (7.18)$$

which yields the *classical* action solution. As we see the Hamilton-Jacobi equation is an autonomous equation which can be solved by just using the knowledge of the behaviour of the potential in the neighbourhood of the periodic orbit. We note that the potential only occurs in this equation. Having found the solution $S(x, t)$ to the Hamilton-Jacobi equation, the amplitude (which we now allow to be complex) fulfills

$$\partial_t \varphi + \nabla \varphi \nabla S + \frac{1}{2} \varphi \Delta S - \frac{i\hbar}{2} \Delta \varphi = 0. \quad (7.19)$$

It is *this* partial differential equation that corresponds to the local path sum (7.8). It is driven by the solution of the Hamilton-Jacobi equation and should be solved in the neighborhood of a periodic orbit with the action expanded like in (7.6).

If the local Schrödinger equation around the periodic orbit has an eigenenergy E the corresponding eigenfunction fulfills

$$\psi_p(t + T_p) = e^{-iET_p/\hbar} \psi_p(t). \quad (7.20)$$

For a general energy value E , the eigenfunctions of the local Hamiltonian $\psi_p^l(t)$ fulfill

$$\psi_p^l(t + T_p) = e^{-iET_p/\hbar} \lambda_p^l(E) \psi_p^l(t). \quad (7.21)$$

where $\lambda_p^l(E) = \exp(i(E - E_l)T_p/\hbar)$. If the eigenvalues $\lambda_p^l(E)$ are known, the local functional determinant (7.12) can be formally written as

$$\Delta_p(E) = \prod_l (1 - \lambda_p^l(E)), \quad (7.22)$$

since $\Delta_p(E) = 0$ yields the eigenenergies of the local Schrödinger problem. We can insert the ansatz (7.16) and reformulate (7.21) as

$$e^{\frac{i}{\hbar}S(t+T_p)} \varphi_p^l(t + T_p) = e^{-iET_p/\hbar} \lambda_p^l(E) e^{\frac{i}{\hbar}S(t)} \varphi_p^l(t). \quad (7.23)$$

The phase change is given by the action integral for one period $S(t+T_p) - S(t) = \int_0^{T_p} L(t) dt$. Using this and the identity for the reduced action $S_p(E)$ of the periodic orbit

$$S_p(E) = \oint pdq = \int_0^{T_p} L(t) dt + ET_p, \quad (7.24)$$

we get

$$e^{\frac{i}{\hbar}S_p(E)}\varphi_p^l(t+T_p) = \lambda_p^l(E)\varphi_p^l(t). \quad (7.25)$$

Introducing the eigenequation for the amplitude

$$\varphi_p^l(t+T_p) = R_p^l(E)\varphi_p^l(t), \quad (7.26)$$

the local spectral determinant can be expressed as

$$\Delta_p(E) = \prod_l (1 - R_p^l(E)e^{\frac{i}{\hbar}S_p(E)}). \quad (7.27)$$

To get the full spectral determinant we therefore have to solve the equation (7.26) in order to get the local eigenvalues. As we shall see this equation can be easily solved on an analytic basis.

We can also reexpress the quantum Gutzwiller-Voros spectral determinant in terms of the local eigenvalues. This reads

$$\Delta(E) = \prod_p \prod_l (1 - R_p^l(E)e^{\frac{i}{\hbar}S_p(E)}). \quad (7.28)$$

The trace formula can be recovered from (7.11):

$$\begin{aligned} \text{Tr}G(E) &= \frac{1}{i\hbar} \sum_p \sum_l \frac{R_p^l(E)e^{\frac{i}{\hbar}S_p(E)}}{1 - R_p^l(E)e^{\frac{i}{\hbar}S_p(E)}} \\ &\times \left(T_p(E) - i\hbar \frac{d \log R_p^l(E)}{dE} \right). \end{aligned} \quad (7.29)$$

To keep an overview over the work that is to be done, it seems appropriate at this point to emphasize an outline over the steps we are going to pursue in the following:

1. First of all we have to solve the local Hamilton Jacobi equation (7.18), in order to be able to drive the amplitude transport equation. This is done by expanding the phase function in a Taylor series, inserting this into the Hamilton-Jacobi equation, and solve the resulting ordinary differential equations.
2. Next we should solve the amplitude transport equation (7.19). This is basically done by using the same strategy as with the phase function, i.e. by expanding the amplitude in a Taylor series around the periodic orbit and solving the ordinary differential equations obtained after insertion into the amplitude equation. However, the $i\hbar\Delta$ term in (7.19) suggest us to expand the Taylor coefficients in a polynomial series in \hbar . Having done

this, we then solve the amplitude equation in two steps: first we solve the *autonomous set* of *semiclassical* equations where we set $\hbar = 0$. Next we can solve the equation recursively to any desired order in \hbar by inserting the previously obtained solutions and keeping the term $i\hbar\Delta$, that connect different orders in \hbar .

3. Now we can concentrate on our main point, namely to solve equation (7.26). By also expanding the local eigenvalues R_l in a powerseries in \hbar and inserting this in the eigenvalue equation (7.26), we can, by comparing terms of same order in \hbar , solve for the R_l coefficients in the expansion of the eigenvalues. This again defines an iterative scheeme, where we can get the \hbar corrections to the eigenvalues by successively inserting the previous found solutions of the eigenvalue equation to lower orders in \hbar .
4. Having found the \hbar corrections of the local eigenvalue problem, we can now get an \hbar corrected local spectral determinant for each periodic orbit, by using (7.27). Multiplying these together we finally end up with an \hbar corrected spectral determinant according to (7.28), or we can get an \hbar corrected trace formula from (7.29).

Solving the equations (7.18-7.19) and (7.26) can be done by a variety of numerical methods. The analytic perturbation method we develop here, can be easily applied also in numerical calculations.

7.3 Analytic eigenbasis

To get the local eigenvalues we have to solve the Hamilton-Jacobi- and the amplitude equations (7.18) (7.19) in order to follow the evolution of a wavepacket around the periodic orbit. In this section we show how the Hamilton-Jacobi equation and the amplitude equation can be solved by changing them into *ordinary* differential equations. For simplicity we shall keep the derivation in one dimension but as we shall demonstrate later the equations are easily obtained in higher dimensions as well.

The Hamilton-Jacobi equation

In the saddlepoint approximation of the trace (7.8) we expressed the phase function S in a powerseries form to get a sum over the local traces. In the neighborhood of a classical periodic orbit we can therefore look for the solution of the Hamilton-Jacobi equation in a power series form. Let $x_p(t)$ denote a classical periodic orbit with period T_p . Let us expand the phase around the time dependent trajectory as in (7.6). To derive ordinary differential equations for the expansion coefficients we expand also the potential around the periodic

orbit

$$U(x) = \sum_{\mathbf{n}}^{\infty} u_{\mathbf{n}}(t)(x - x_p(t))^{\mathbf{n}} / \mathbf{n}!, \quad (7.30)$$

where $u_{\mathbf{n}}$ are rank n tensors in general. If we put these two expressions into the Hamilton-Jacobi equation we get in the one-dimensional case

$$\dot{s}_n - s_{n+1}\dot{q} + \frac{1}{2} \sum_{l=0}^n \frac{n!}{(n-l)!l!} s_{n-l+1}s_{l+1} + u_n = 0 \quad (7.31)$$

which represents a hierarchy of equations. In the multidimensional case we get similar expressions for the entries of the s matrices. In the Hamilton-Jacobi equation it is common to interpret the gradient of the phase function as the momentum. If the s_1 vector is chosen to be the momentum of the classical orbit

$$p = \dot{q} = s_1, \quad (7.32)$$

the equations are simpler and their meanings are obvious. The first equation in the hierarchy corresponds to the classical action along the path:

$$\dot{s}_0 = \frac{p^2}{2} - u_0 = L(t), \quad (7.33)$$

where $L(t)$ is the Lagrange function evaluated on the periodic orbit. The second is the Newton equation

$$\dot{p} = -u_1, \quad (7.34)$$

since u_1 is the force along the trajectory. The $d \times d$ matrix s_2 is familiar from the wave packet theory and describes the shape of a Gaussian wave packet[37]

$$\dot{s}_2 = -s_2^2 - u_2. \quad (7.35)$$

We earlier encountered this equation in (5.22) where we studied the time evolution of the curvature matrix \mathbf{M} . Equation (7.35) is simply the one dimensional version of this evolution equation for the curvature matrix, which in this case is just the Sinai Bunimovic curvature. We therefore also know that $\text{Tr} s_2$ describes the expansion of infinitesimal volume elements evolving along the classical orbit. The next equation

$$\dot{s}_3 = -3s_2s_3 - u_3, \quad (7.36)$$

and the rest of the equations are linear equations for s_n . These are pure classical equations describing the analytic structure of the action around the periodic orbits p .

Since the phase change along the periodic orbit is just given by the action integral (7.24), the gradient of $S(x, t)$ entering in the amplitude equation (7.19) must be a periodic function along the periodic orbit. Therefore, the $s_n, n > 0$ matrices are also periodic yielding the boundary conditions $s_n(t) = s_n(t + T_p)$ where T_p is the period of the orbit. The term $s_0(t)$ given by the action integral $s_0(t) = \int_0^t L(t)dt$ is then not periodic whereas for instance the momentum $s_1(t)$ along the periodic orbit varies periodically with time. The most complicated equation we have to solve is (7.35). In general it has more than one periodic solution. In case of unstable periodic orbits the solution of the equation (7.35) converges to a single stable solution starting from almost all initial conditions. A simple example of this can be obtained by considering the periodic orbit ‘0’ of the 3-disk system. This has the Jacobian:

$$\mathbf{J}_0 = \begin{bmatrix} 1 & 4 \\ 2 & 9 \end{bmatrix}. \quad (7.37)$$

The rational fraction transformation (5.20) in this case yields

$$f(s_2) = \frac{2 + 9s_2}{1 + 4s_2} \quad (7.38)$$

and starting from almost any point this converges after a few iterations to the stable solution $s_2 = f(s_2) = 2.22474487\dots$. The rest of the solutions are unstable. The wave packet described by the stable solution is decaying in time, while the rest of the solutions describe wave packets with increasing amplitudes. These solutions are non-physical, since they describe local wave functions with exponentially increasing norms. We have to exclude these solutions. In case of stable periodic orbits we also have only one solution of (7.35) for which the local wave function is decaying and we have to choose this solution. The higher order ($n > 2$) equations are linear in s_n and their unique periodic solutions can be found order by order.

The evolution of the amplitude

After solving locally the Hamilton-Jacobi equation we can look for the local solution of the amplitude equation. In a similar way as with the phase function, we can expand the amplitude around the classical path in power series. This analytic basis is appropriate for classical Perron-Frobenius operators since it is very easy to diagonalize the evolution operator on this basis[47]. Inserting the expansion

$$\varphi_p(x, t) = \sum_{\mathbf{n}}^{\infty} \varphi_{\mathbf{n}}(t) (x - x_p(t))^{\mathbf{n}} / \mathbf{n}! \quad (7.39)$$

into the equation (7.19) yields in one dimension the following equations for the coefficients

$$\dot{\varphi}_n - \varphi_{n+1} \dot{q} + \sum_{l=0}^n \frac{n!}{(n-l)!l!} \left(\varphi_{n-l+1} s_{l+1} + \frac{1}{2} \varphi_{n-l} s_{l+2} \right)$$

$$-\frac{i\hbar}{2}\varphi_{n+2} = 0. \quad (7.40)$$

Note that the term $i\hbar/2\varphi_{n+2}$ connects different orders in \hbar .

In the multidimensional case we get similar equations for the expansion coefficient matrices. Using eq. (7.32) one can slightly reduce these equations:

$$\begin{aligned}\dot{\varphi}_0 &= -\frac{s_2}{2}\varphi_0 + \frac{i\hbar}{2}\varphi_2 \\ \dot{\varphi}_1 &= -\frac{3s_2}{2}\varphi_1 - \frac{s_3}{2}\varphi_0 + \frac{i\hbar}{2}\varphi_3 \\ \dot{\varphi}_2 &= -\frac{5s_2}{2}\varphi_2 - 2s_3\varphi_1 - \frac{s_4}{2}\varphi_0 + \frac{i\hbar}{2}\varphi_4\end{aligned} \quad (7.41)$$

and so on. These equations are linear and have the general form

$$\dot{\varphi}_n = -\frac{(2n+1)s_2}{2}\varphi_n \dots + \frac{i\hbar}{2}\varphi_{n+2}. \quad (7.42)$$

In the semiclassical limit where we can set $\hbar = 0$, we see that the hierarchy of equations take the form

$$\dot{\varphi} = \mathbf{T}\varphi \quad (7.43)$$

where \mathbf{T} is a lower triangular matrix. This means that the solutions φ^l can be found successively by setting all $\varphi_i^l = 0$ for $i < l$. In the case of higher dimensions this still holds but the indexation is more tedious, since the equations are matrix equations in higher dimensions. However the structure of the hierarchy of equations remain the same in any number of dimensions.

7.4 Stationary solutions

The set of equations (7.31), (7.40) and (7.26) define the full set of equations we have to solve. Furthermore we know, that we are seeking the stationary solutions of the Schrödinger equation. The stationarity condition implies that the phase of the wave function fulfills the condition

$$\frac{\partial S(x, t)}{\partial t} = -E, \quad (7.44)$$

and the amplitude has no *explicit* time dependence

$$\frac{\partial \varphi(x, t)}{\partial t} = 0. \quad (7.45)$$

These equations give us additional equations for the expansion coefficients, which have the form

$$\dot{s}_0(t) - \dot{q}(t)s_1(t) = -E, \quad (7.46)$$

$$\dot{s}_n(t) - \dot{q}(t)s_{n+1}(t) = 0 \quad \text{for } n > 0, \quad (7.47)$$

$$\dot{\varphi}_n(t) - \dot{q}(t)\varphi_{n+1}(t) = 0 \quad \text{for } n \geq 0, \quad (7.48)$$

in the one-dimensional case. In the multidimensional case the coefficient matrices fulfill similar equations. These equations can help us to reduce the number of equations that we have to solve, since some of the higher order expansion coefficients can be expressed by the time derivatives of the lower order coefficients. In one dimension all the higher coefficients can be directly computed from the time derivatives of the zero order terms. In two dimensions the number of s_n and φ_n matrix elements is $n + 1$. For example we need the $4 = 3 + 1$ coefficients $S_{x^3}, S_{x^2y}, S_{xy^2}, S_{y^3}$ in the Taylor expansion of the phase function to the $n = 3$ 'rd order. The number of the additional equations derived above is n . Therefore, on each level we need to solve 1 new equation. In three dimensions we get n entirely new equations for the phase and the amplitude on each level. In section 7.7 we show how the reduction of the equations can be carried out.

7.5 \hbar expansion in the analytic base

As we saw in (7.40) the amplitude equation expanded in the analytical basis yields a coupling between different orders of \hbar . Since \hbar is a small parameter we can develop a perturbation series for the amplitudes

$$\varphi^l(t) = \sum_{m=0}^{\infty} \left(\frac{i\hbar}{2}\right)^m \varphi^{l(m)}(t) \quad (7.49)$$

which we can then insert into the equation (7.40 -7.42). This results in a tower of coupled equations. In this section we discuss the semiclassical or zeroth order in \hbar of these equations whereas the coupling to higher orders in \hbar which yields the \hbar corrections, will be discussed in the next section. The zeroth order or semiclassical equations form an autonomous system

$$\begin{aligned} \dot{\varphi}_n^{(0)} - \varphi_{n+1}^{(0)} \dot{q} &+ \sum_{l=0}^n \frac{n!}{(n-l)!l!} \left(\varphi_{n-l+1}^{(0)} s_{l+1} + \frac{1}{2} \varphi_{n-l}^{(0)} s_{l+2} \right) \\ &= 0. \end{aligned} \quad (7.50)$$

For example, the first three equations have the form

$$\begin{aligned} \dot{\varphi}_0^{(0)} &= -\frac{s_2}{2} \varphi_0^{(0)}, \\ \dot{\varphi}_1^{(0)} &= -\frac{3s_2}{2} \varphi_1^{(0)} - \frac{s_3}{2} \varphi_0^{(0)}, \\ \dot{\varphi}_2^{(0)} &= -\frac{5s_2}{2} \varphi_2^{(0)} - 2s_3 \varphi_1^{(0)} - \frac{s_4}{2} \varphi_0^{(0)}. \end{aligned} \quad (7.51)$$

The important feature of these equations is that they are linear and have the general form

$$\dot{\varphi}_n^{(0)} = -\frac{(2n+1)s_2}{2} \varphi_n^{(0)} + \dots, \quad (7.52)$$

and so on. We note that this hierarchy of equations has the same structure as (7.43) and can therefore be solved in the same fashion, i.e. by successively putting the low order $n < l$ equal to zero in order to get the l 'th eigen function.

Now the eigenvalue $R_l(E)$ which it is our main task to obtain, can also be expanded in powers of $i\hbar/2$:

$$R_l(E) = \exp \left\{ \sum_{m=0}^{\infty} \left(\frac{i\hbar}{2} \right)^m C_l^{(m)} \right\}. \quad (7.53)$$

Expanding the exponential yields

$$R_l(E) = \exp(C_l^{(0)}) \left(1 + \frac{i\hbar}{2} C_l^{(1)} \left(\frac{i\hbar}{2} \right)^2 \left(\frac{1}{2}(C_l^{(1)})^2 + C_l^{(2)} \right) + \dots \right) \quad (7.54)$$

The eigenvalue equation (7.26) in \hbar expanded form now reads

$$\begin{aligned} \sum_{m=0}^{\infty} \left(\frac{i\hbar}{2} \right)^m \varphi^{l(m)}(t + T_p) &= \\ \exp \left\{ \sum_{m=0}^{\infty} \left(\frac{i\hbar}{2} \right)^m C_l^{(m)} \right\} \cdot \sum_{m=0}^{\infty} \left(\frac{i\hbar}{2} \right)^m \varphi^{l(m)}(t). \end{aligned} \quad (7.55)$$

Expanding the eigenvalue like in (7.54) and collecting the terms of the same order in \hbar yield a set of eigenequations

$$\begin{aligned} \varphi^{l(0)}(t + T_p) &= \exp(C_l^{(0)}) \varphi^{l(0)}(t), \\ \varphi^{l(1)}(t + T_p) &= \exp(C_l^{(0)}) [\varphi^{l(1)}(t) + C_l^{(1)} \varphi^{l(0)}(t)], \\ \varphi^{l(2)}(t + T_p) &= \exp(C_l^{(0)}) [\varphi^{l(2)}(t) + C_l^{(1)} \varphi^{l(1)}(t) \\ &\quad + (C_l^{(2)} + \frac{1}{2}(C_l^{(2)})^2) \varphi^{l(0)}(t)], \end{aligned} \quad (7.56)$$

and so on. These equations are the conditions selecting the eigenvectors and eigenvalues and they hold for all t . Without loss of generality we can also assume that $\varphi^{l(0)}(0) = 1$ and $\varphi^{l(m)}(0) = 0$ for $m > 0$. By adding these assumptions we can simplify the equations (7.56):

$$\begin{aligned} \varphi^{l(0)}(T_p) &= \exp(C_l^{(0)}), \\ \varphi^{l(1)}(T_p) &= \exp(C_l^{(0)}) C_l^{(1)}, \\ \varphi^{l(2)}(T_p) &= \exp(C_l^{(0)}) (C_l^{(2)} + \frac{1}{2}(C_l^{(2)})^2). \end{aligned} \quad (7.57)$$

Now by solving the first of these equations (7.51) we get

$$\varphi_0^{0(0)}(t) = \varphi_0^{0(0)}(0) \exp \left(- \int_0^t \frac{1}{2} s_2(t) dt \right). \quad (7.58)$$

By using (7.57) we can read off the zeroth eigenvalue

$$C_0^{(0)} = - \int_0^{T_p} \frac{1}{2} s_2(t) dt. \quad (7.59)$$

The s_2 in general goes through $1/t$ type singularities. If this happens the integral should be carried out by principal value integration, as we saw in section ??.

The rest of the equations do not play a role in yielding the first eigenvalue. The solution $\varphi_0^{(0)}(t)$ can be inserted into the next equation (7.51). Since equation (7.51) is a linear one driven by $\varphi_0^{(0)}(t)$ its particular solution fulfills the condition (7.56). The rest of the equations can be solved the same way and we get the eigenamplitudes $\varphi_n^{(0)}$. The rest of the semiclassical eigenvalues $R_l(E)$, $l > 0$ can be recovered by setting $\varphi_n^{(0)} = 0$ for $n < l$ since the system of equations has the upper triangular structure as we saw in the previous section. Then the l -th semiclassical eigenvalue is given by

$$C_l^{(0)} = -\frac{2l+1}{2} \int_0^{T_p} s_2(t) dt. \quad (7.60)$$

The semiclassical eigenvalues are connected with the stability properties of the periodic orbits. For example the first ($l = 0$) eigenvalue is related to the product of the expanding eigenvalues[53]

$$\exp(C_0^{(0)}) = \frac{e^{i\mu_p \pi}}{|\prod_i \Lambda_i|^{1/2}} \quad (7.61)$$

and in the general l case we obtain

$$\exp(C_l^{(0)}) = \frac{e^{i\mu_p \pi}}{|\prod_i \Lambda_i|^{1/2} (\prod_i \Lambda_i)^l} \quad (7.62)$$

where Λ_i denotes the expanding ($\Lambda_i > 1$) eigenvalues of the linear stability or Jacobi matrix of the periodic orbit and ν_p is the Maslov index of the periodic orbit. The Maslov phase comes from the singularities of $s_2(t)$ (see ref.[53].) The product

$$\begin{aligned} \Delta(E) &= \prod_p \prod_l (1 - \exp(iS_p/\hbar + C_l^{(0)})) \\ &= \prod_p \prod_{l=0}^{\infty} \left(1 - \frac{\exp(iS_p/\hbar + i\mu_p \pi)}{|\prod_i \Lambda_i|^{1/2} (\prod_i \Lambda_i)^l}\right) \end{aligned} \quad (7.63)$$

in this approximation is the previously obtained Gutzwiller-Voros zeta function.

7.6 The \hbar correction equations

By following the strategy outlined in section (7.2) we have now finished the semiclassical part where we put $\hbar = 0$ in all the equations. As we have demonstrated we end up (not surprisingly) with the usual Gutzwiller Voros results.

After the calculation of the local semiclassical eigenvalues and eigenvectors we can now concentrate on the main item: to find \hbar corrections to the semiclassical eigenvalues. As mentioned in section (7.2) we can use the semiclassical results to find the first \hbar correction by inserting them in the next level of approximation.

The differential equations connecting the $m + 1$ -th order amplitudes with the m -th order amplitudes are

$$\begin{aligned} \dot{\varphi}_n^{(m+1)} - \varphi_{n+1}^{(m+1)} \dot{q} &+ \\ \sum_{l=0}^n \frac{n!}{(n-l)!l!} \left(\varphi_{n-l+1}^{(m+1)} s_{l+1} + \frac{1}{2} \varphi_{n-l}^{(m+1)} s_{l+2} \right) - \varphi_{n+2}^{(m)} &= 0. \end{aligned} \quad (7.64)$$

which we get from the original amplitude equations (7.19), or (7.40) which still contains the \hbar term. Again, using (7.32) we can reduce these equations

$$\begin{aligned} \dot{\varphi}_0^{(m+1)} &= -\frac{s_2}{2} \varphi_0^{(m+1)} + \varphi_2^{(m)}, \\ \dot{\varphi}_1^{(m+1)} &= -\frac{3s_2}{2} \varphi_1^{(m+1)} - \frac{s_3}{2} \varphi_0^{(m+1)} + \varphi_3^{(m)}, \\ \dot{\varphi}_2^{(m+1)} &= -\frac{5s_2}{2} \varphi_2^{(m+1)} - 2s_3 \varphi_1^{(m+1)} - \frac{s_4}{2} \varphi_0^{(m+1)} + \varphi_4^{(m)}, \end{aligned} \quad (7.65)$$

and so on. These equations are linear and have the general form

$$\dot{\varphi}_n^{(m+1)} = -\frac{(2n+1)s_2}{2} \varphi_n^{(m+1)} + \dots + \varphi_{n+2}^{(m)}. \quad (7.66)$$

Inserting the eigenamplitudes $\varphi_n^{l(m)}(t)$ we get linear driven equations for the next order of the amplitudes. The solutions of these equations, which satisfy the conditions of type (7.56), yield the corrections $C_l^{(m)}$ of the semiclassical eigenvalues $C_l^{(0)}$.

In the following we just want to calculate the first \hbar correction $C_l^{(1)}$ to the eigenvalues R_l . To do this we have to proceed in the following way

1. First we observe from (7.57) that $C_l^{(1)}$ can be obtained if we can find $\varphi^{l(1)}(t)$. More precisely, it suffices to find $\varphi_0^{l(1)}(t)$ since all the expansion coefficients in $\varphi^{l(1)}$ decays with the same ratio during one period. This means that we just have to solve equation (7.65) with $m = 0$.
2. From equation (7.65) we see that this implies that we need $\varphi_2^{l(0)}$, that is, the zeroth order in \hbar or semiclassical solution of the l 'th eigenfunction to the second order in the powerseries expansion. To get this, we then have to solve the equations (7.51 - 7.52) successively for the l 'th eigenfunction.
3. Finally we see from equation (7.52) that the above item 2. requires that we solve the Hamilton-Jacobi equation (7.18) up to fourth order to provide us with s_1, s_2, s_3 and s_4 .

In the following we shall refer to the above list as the *prescription* to obtain the first order \hbar correction to the local eigenvalues. Of course, to get the first \hbar correction, one should start from the last item and finally end up with

$$C_l^{(1)} = \frac{\varphi^{l(1)}(T_p)}{\exp(C_l^{(0)})}. \quad (7.67)$$

The higher order \hbar corrections can be found in a similar fashion by observing which ingredients are needed in equation (7.57) to provide us with $C_l^{(2)}$ and so on.

As a consequence of the above hierarchy of equations one has to solve, it is increasingly difficult to get corrections to the eigenvalues corresponding to large l . It is more convenient to reorganize the quantum Selberg product as a product of quantum inverse zeta functions

$$\Delta(E) = \prod_l \zeta_l^{-1}(E) \quad (7.68)$$

where the quantum zeta functions are defined by

$$\zeta_l^{-1}(E) = \prod_p \left(1 - \exp(iS_p(E)/\hbar + \sum_m (i\hbar/2)^m C_l^{p(m)}(E)) \right). \quad (7.69)$$

These zeta functions are the quantum generalizations of the Ruelle zeta functions[45, 3]. The leading resonances and the eigenenergies can be computed from the zeroes of the $l = 0$ quantum zeta function. The curvature expansion explained in section (3.1) can also be applied using the new quantum mechanical weights

$$t_p = \exp \left(iS_p(E)/\hbar + \sum_m (i\hbar/2)^m C_0^{p(m)}(E) \right). \quad (7.70)$$

In the next section we show how the method can be applied to obtain the first \hbar correction $C_l^{(1)}$ in the case of two-dimensional billards.

7.7 Billards

To apply the theory on billiard systems we first have to discuss some special features of these systems. In billiards the potential is not an analytic function: the Dirichlet boundary condition for the wave function on a hard wall implies that the wave function should vanish on the wall. Our approach here is basically to trace a wave packet along the classical trajectory in the configuration space. When the packet hits the wall, the incoming wave function at time t is given by the packet right before the collision, evaluated on the wall

$$\psi_{in}(x(s), y(s), t) = \varphi(x(s), y(s), t_{-0}) e^{iS((x(s), y(s), t_{-0}))/\hbar}, \quad (7.71)$$

where $(x(s), y(s))$ is some analytic parametrization of the wall around the classical point of reflection. The outgoing wave function is the wave function right after the collision

$$\psi_{out}(x(s), y(s), t) = \varphi(x(s), y(s), t_{+0}) e^{iS((x(s), y(s), t_{+0}))/\hbar}. \quad (7.72)$$

The sum of the incoming and the outgoing wave functions should vanish on the hard wall due to the Dirichlet condition. This implies that the incoming and the outgoing amplitude and the phase are related by

$$\varphi(x(s), y(s), t_{-0}) = \varphi(x(s), y(s), t_{+0}) \quad (7.73)$$

$$S(x(s), y(s), t_{-0}) = S(x(s), y(s), t_{+0}) + i\pi. \quad (7.74)$$

These relations mean that the power series with respect to s of these functions are equal on both sides of the collision modulo the π phase shift. This phase shift can be interpreted as the Maslov phase coming from the hard wall.

The stationarity conditions for billards

In this paragraph we derive the stationarity conditions (7.44) and (7.45) for the special case two-dimensional of billards. We start by introducing the notation

$$\begin{aligned} \Delta x^n &= (x - q_x(t))^n \\ \Delta y^m &= (y - q_y(t))^m \end{aligned} \quad (7.75)$$

where $(q_x(t), q_y(t))$ denotes the classical trajectory of the particle. We can then expand the phase function $S(x, y, t)$ as

$$\begin{aligned} S(x, y, t) &= S_0 + S_x \Delta x + S_y \Delta y \\ &+ \frac{1}{2} (S_{x^2} \Delta x^2 + 2S_{xy} \Delta x \Delta y + S_{y^2} \Delta y^2) \\ &+ \dots \end{aligned} \quad (7.76)$$

By choosing the right hand orientated coordinate system so that the x axis is directed along the particle trajectory we can already simplify the equations considerably since we then have

$$\begin{aligned} S_x &= \dot{q}_x = 1 \\ S_y &= \dot{q}_y = 0 \end{aligned} \quad (7.77)$$

because the gradient of the phase function is just equal to the momentum which we have set to be of unit size. From the general stationarity conditions (7.44) and (7.45) we then get

$$\begin{aligned} \frac{\partial S}{\partial t} &= \dot{S}_0 - \dot{q}_x S_x - \dot{q}_y S_y \\ &+ (\dot{S}_x - S_{x^2} \dot{q}_x - S_{xy} \dot{q}_y) \Delta x \\ &+ (\dot{S}_y - S_{xy} \dot{q}_x - S_{y^2} \dot{q}_y) \Delta y \\ &+ \dots \\ &= -E. \end{aligned} \quad (7.78)$$

From this we get by using (7.77) the relations

$$\begin{aligned}\dot{S}_0 - \dot{q}_x S_x &= -E \\ \dot{S}_x - S_{x^2} \dot{q}_x &= 0 \\ \dot{S}_y - S_{xy} \dot{q}_x &= 0\end{aligned}\tag{7.79}$$

where the last two relations can also be written

$$\begin{aligned}S_{x^2} &= 0 \\ S_{xy} &= \frac{\dot{S}_y}{S_x}\end{aligned}\tag{7.80}$$

since $\dot{S}_x = 0$ and $S_x = \dot{q}_x$. In general we get to order $\Delta x^n \Delta y^m$ where $n+m > 0$:

$$\begin{aligned}\frac{\partial S}{\partial t}|_{\Delta x^n \Delta y^m} &= \frac{1}{(n+m)!} \left[\binom{n+m}{n} \dot{S}_{x^n y^m} - \dot{q}_y (m+1) \binom{n+m+1}{n} S_{x^n y^{m+1}} \right. \\ &\quad \left. - \dot{q}_x (n+1) \binom{n+m+1}{m} S_{x^{n+1} y^m} \right] \\ &= 0\end{aligned}\tag{7.81}$$

which by use of (7.77) gives the stationarity conditions

$$S_{x^{n+1} y^m} = \frac{\dot{S}_{x^n y^m}}{S_x}.\tag{7.82}$$

For the amplitude everything works in exactly the same fashion and we get

$$\varphi_{x^{n+1} y^m} = \frac{\dot{\varphi}_{x^n y^m}}{S_x}.\tag{7.83}$$

for all orders $n+m \geq 0$.

The Hamilton-Jacobi equation for billiards

In order to solve the Hamilton-Jacobi equation along the periodic orbit we shall in the following first investigate how the phases change in the case of a bounce on the hard walls. Here we keep the calculation in two dimensions but the generalization to higher dimensions follows the same strategy. We start by expanding the phase function S around the periodic orbit in the neighbourhood of the bouncing point. The expansion must be to the fourth order since we need this in order to solve equation (7.52) according to the 3'rd item in the prescription. The expansion then reads:

$$\begin{aligned}S(x, y; t) &= S_0 + S_x x + S_y y \\ &\quad + \frac{1}{2!} (S_{xx} x^2 + 2S_{xy} xy + S_{yy} y^2) \\ &\quad + \frac{1}{3!} (S_{xxx} x^3 + 3S_{xxy} x^2 y + 3S_{xyy} x y^2 + S_{yyy} y^3) \\ &\quad + \frac{1}{4!} (S_{xxxx} x^4 + 4S_{xxxy} x^3 y + 6S_{xxyy} x^2 y^2 + 4S_{xyyy} x y^3 + S_{yyyy} y^4) \\ &\quad + \dots\end{aligned}\tag{7.84}$$

Here x and y are shorthand notations for the previously introduced notation $x = \Delta x = (x - q_x(t))$ and $y = \Delta y = (y - q_y(t))$, i.e. the deviations from the periodic orbit at time t in a right hand orientated coordinate systems with x -axis in to the momentum direction. According to the stationarity conditions (7.82) some of these terms are zero so we get:

$$\begin{aligned} S(x, y; t) &= S_0 + S_x x \\ &+ \frac{1}{2!} S_{yy} y^2 \\ &+ \frac{1}{3!} (3S_{xyy} xy^2 + S_{yyy} y^3) \\ &+ \frac{1}{4!} (6S_{xxyy} x^2 y^2 + 4S_{xyyy} xy^3 + S_{yyyy} y^4). \end{aligned} \quad (7.85)$$

We should of course work with two such expansions, one corresponding to the incoming wave packet, which we shall denote S^- , and an expansion S^+ corresponding to the outgoing wave. Consequently we also have two different coordinate representations (x^{in}, y^{in}) and (x^{out}, y^{out}) each of which are right hand orientated and with the x -axis in the momentum direction. It is in these coordinates that S^- and S^+ should be expanded. The two expansions S^- and S^+ should then coincide locally on the wall at the bouncing point. In the general case the wall is determined locally by the set of points $\{(x, y) | x(y) = C_2 y^2 / 2! + C_3 y^3 / 3! + C_4 y^4 / 4!\}$, where (x, y) now denotes a local intermediate coordinate system with y -axis tangent to the wall at the bouncing point. The geometry of the entire construction is shown in figure 7.1. It is in

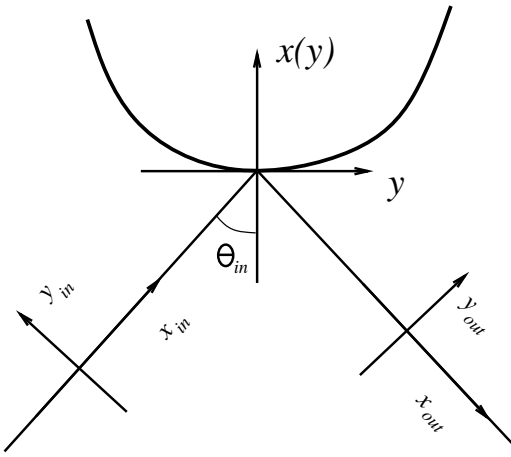


Figure 7.1: The coordinate systems introduced.

the local intermediate coordinates that we shall make the incoming and outgoing phase function coincide.

The incoming and outgoing coordinate systems are given by the set of transformation equations:

$$\begin{aligned} x^{in} &= \cos \theta x + \sin \theta y \\ y^{in} &= \sin \theta x - \cos \theta y \end{aligned} \quad (7.86)$$

and

$$\begin{aligned} x^{out} &= -\cos \theta x + \sin \theta y \\ y^{out} &= \sin \theta x + \cos \theta y. \end{aligned} \quad (7.87)$$

As mentioned, the transformations are chosen in order to get $S_x = p$ both before and after the bounce, and so that all the coordinate systems are right hand orientated. Taking each of the terms in (7.86) and expanding them in terms of the intermediate $(x(y), y)$ yields

$$\begin{aligned} x^{in} &= \sin \theta y + \cos \theta [C_2 y^2 / 2! + C_3 y^3 / 3! + C_4 y^4 / 4! + \dots] \\ y^{in} &= -\cos \theta y + \sin \theta [C_2 y^2 / 2! + C_3 y^3 / 3! + C_4 y^4 / 4! + \dots]. \end{aligned}$$

Now, by expanding S^- and S^+ in the *intermediate* coordinate system, and by comparing terms of same order in y we can get the equations that describes the discontinuous change of the expansion coefficients at the bouncing point. To the second order in y we get:

$$S_x \cos \theta \frac{C_2}{2} + \frac{1}{2!} S_{yy}^- \cos^2 \theta = -S_x \cos \theta \frac{C_2}{2} + \frac{1}{2!} S_{yy}^+ \cos^2 \theta \quad (7.88)$$

which just yields the usual formula (6.41) for the Sinai-Bunimovich curvature:

$$S_{yy}^+ = S_{yy}^- + \frac{2C_2}{\cos \theta}. \quad (7.89)$$

To the third order in y we get :

$$\begin{aligned} S_{yyy}^+ &= -S_{yyy}^- + \frac{2C_3 S_x}{\cos^2 \theta} \\ &- \frac{3 \sin \theta}{\cos^2 \theta} C_2 (S_{yy}^- + S_{yy}^+) \\ &+ \frac{3 \sin \theta}{\cos \theta} (S_{xyy}^- - S_{xyy}^+), \end{aligned} \quad (7.90)$$

and finally we get to the fourth order of y :

$$\begin{aligned} S_{yyyy}^+ &= S_{yyyy}^- \\ &- 4 \frac{\sin \theta}{\cos \theta} (S_{xyyy}^- + S_{xyyy}^+) \\ &+ 6 \frac{\sin^2 \theta}{\cos^2 \theta} (S_{xxyy}^- - S_{xxyy}^+) \\ &+ 6 \frac{\sin \theta}{\cos^2 \theta} C_2 (S_{yyy}^- - S_{yyy}^+) \\ &+ 12 \left(\frac{1}{2 \cos \theta} - \frac{\sin^2 \theta}{\cos^3 \theta} \right) C_2 (S_{xyy}^- + S_{xyy}^+) \\ &+ 3 \frac{\sin^2 \theta}{\cos^4 \theta} C_2^2 (S_{yy}^- - S_{yy}^+) \\ &- 4 \frac{\sin \theta}{\cos^3 \theta} C_3 (S_{yy}^- + S_{yy}^+) \\ &+ \frac{2C_4}{\cos^3 \theta}. \end{aligned} \quad (7.91)$$

As we see, the result of the discontinuous bounce evolution is still not a closed expression. In addition we should also obtain the bouncing rules for the mixed derivatives. This is accomplished by applying the stationarity conditions (7.82). For instance we have

$$S_{xyy} = \frac{\dot{S}_{yy}}{S_x} = -\frac{S_{yy}^2}{S_x},$$

which gives us

$$S_{xyy}^+ = -\frac{(S_{yy}^- + \frac{2C_2}{\cos \theta})^2}{S_x}, \quad (7.92)$$

and similarly we get

$$S_{xyy} = \frac{\dot{S}_{yyy}}{S_x} = -\frac{3S_{yy}S_{yyy}}{S_x},$$

and

$$S_{xxyy} = \frac{\dot{S}_{xyy}}{S_x} = \frac{\ddot{S}_{yy}}{S_x^2} = -\frac{\dot{S}_{yy}^2}{S_x^2} = \frac{2S_{yy}^3}{S_x^2}.$$

This concludes our derivation of the discontinuous evolution of the coefficients $S_{x^n y^m}$, at the bouncing points.

To derive the continuous time evolution we have to solve the Hamilton-Jacobi equations (7.18). Since we can find the mixed coefficients by the stationarity conditions (7.82), we only have to solve for the S_{y^n} coefficients. Inserting the expansion (7.86) into the Hamilton-Jacobi equations (7.18) the equations for these becomes

$$\begin{aligned} \dot{S}_{yy} + S_{yy}^2 &= 0 \\ \dot{S}_{yyy} + 3S_{yy}S_{yyy} &= 0 \\ \dot{S}_{yyyy} + 4S_{yyyyy}S_{yy} + 3S_{yyy}^2 + 3S_{xyy}^2 &= 0. \end{aligned} \quad (7.93)$$

since there is no potential present except for the hard walls. By integration these equations immediately yield

$$\begin{aligned} S_{yy}(t) &= \frac{1}{t + t_0} \\ S_{yyy}(t) &= \frac{A}{(t + t_0)^3} \\ S_{yyyy}(t) &= -\frac{3}{(t + t_0)^3} + \frac{B}{(t + t_0)^4} + \frac{3A^2}{(t + t_0)^5} \end{aligned} \quad (7.94)$$

where the constants are to be determined from the initial values of the coefficients of the phase function. We now have the necessary ingredients for solving the Hamilton-Jacobi equation to the 4'th order: between the bounces we use the continuous time evolution (7.95), and on the bouncing points we use the derived bouncing relations (7.89),(7.90) and (7.91) to follow evolution of the phase function.

The amplitude evolution for billards

Next we need to solve the amplitude equations. As before, we start by looking at the amplitude and how its expansion coefficients change when the wave goes through a bounce. This is done by using exactly the same procedure as outlined above. For simplicity we start by only looking at the 0'th order $l = 0$ eigenfunction. We first expand the amplitude in the same fashion as we expanded the action. According to the second item in the *prescription* we only need the expansion to second order:

$$\varphi(x, y) = \varphi_0 + \varphi_x x + \varphi_y y + \frac{1}{2!}(\varphi_{xx} x^2 + 2\varphi_{xy} xy + \varphi_{yy} y^2) + \dots$$

Here again we actually have two expansions φ^- and φ^+ corresponding to the incomming and the outgoing wavepacket. By comparing the different powers of y in the intermediate coordinate system we get:

$$\varphi_0^+ = \varphi_0^- \quad (7.95)$$

$$\varphi_x^+ \sin \theta + \varphi_y^+ \cos \theta = \varphi_x^- \sin \theta - \varphi_y^- \cos \theta \quad (7.96)$$

for the zeroth and first order, and

$$\begin{aligned} \varphi_x^- \cos \theta \frac{C_2}{2} + \varphi_y^- \sin \theta \frac{C_2}{2} &+ \varphi_{xx}^- \sin^2 \theta \frac{1}{2} - \sin \theta \cos \theta \varphi_{xy}^- + \frac{1}{2} \varphi_{yy}^- \cos^2 \theta = \\ -\varphi_x^+ \cos \theta \frac{C_2}{2} + \varphi_y^+ \sin \theta \frac{C_2}{2} &+ \varphi_{xx}^+ \sin^2 \theta \frac{1}{2} + \sin \theta \cos \theta \varphi_{xy}^+ + \frac{1}{2} \varphi_{yy}^+ \cos^2 \theta \end{aligned}$$

for the second order in y . This gives the set of bounce equations:

$$\begin{aligned} \varphi_0^+ &= \varphi_0^- \\ \varphi_y^+ &= -\varphi_y^- + \tan \theta (\varphi_x^- - \varphi_x^+) \end{aligned} \quad (7.97)$$

and

$$\begin{aligned} \varphi_{yy}^+ &= \varphi_{yy}^- - 2 \tan \theta (\varphi_{xy}^- + \varphi_{xy}^+) + \tan^2 \theta (\varphi_{xx}^- - \varphi_{xx}^+) \\ &+ C_2 \frac{\sin \theta}{\cos^2 \theta} (\varphi_y^- - \varphi_y^+) + \frac{C_2}{\cos \theta} (\varphi_x^- + \varphi_x^+). \end{aligned} \quad (7.98)$$

To reduce these equations further we have to make use of the stationarity equations for the amplitude (7.83). The ones we need are given by

$$\begin{aligned} \dot{\varphi}_0 - \varphi_x S_x &= 0, \\ \dot{\varphi}_x - \varphi_{xx} S_x &= 0, \\ \dot{\varphi}_y - \varphi_{xy} S_x &= 0. \end{aligned} \quad (7.99)$$

These equations together with the semiclassical amplitude equations (7.51 - 7.52) for the φ_{y^n} 's yield the reductions. In the two-dimensional case the semiclassical amplitude equations becomes

$$\dot{\varphi}_0 + \frac{1}{2} S_{yy} \varphi_0 = 0$$

$$\begin{aligned}\dot{\varphi}_y + \frac{3}{2}S_{yy}\varphi_y + \frac{1}{2}S_{yyy}\varphi_0 &= 0 \\ \dot{\varphi}_{yy} + \frac{5}{2}S_{yy}\varphi_{yy} + S_{yyx}\varphi_x &+ \\ 2S_{yyy}\varphi_y + \frac{1}{2}(S_{xxyy} + S_{yyyy})\varphi_0 &= 0\end{aligned}\tag{7.100}$$

Using these equations and the above stationarity conditions we get

$$\varphi_x^{+/-} = \frac{\dot{\varphi}_0^{+/-}}{p} = \frac{-S_{yy}^{+/-}\varphi_0^{+/-}}{2p}.$$

By using this reduction and the previously obtained expressions for the S_y 's we can derive the explicit bouncing relations:

$$\varphi_0^+ = \varphi_0^-, \tag{7.101}$$

$$\varphi_y^+ = -\varphi_y^- + \frac{C_2 \sin \theta}{\cos^2 \theta} \varphi_0. \tag{7.102}$$

Similarly we have

$$\varphi_{xx} = \dot{\varphi}_x = -\frac{1}{2} \frac{d}{dt} S_{yy} \varphi_0 = \frac{3}{4} S_{yy}^2 \varphi_0, \tag{7.103}$$

and

$$\varphi_{xy} = \dot{\varphi}_y = -\frac{1}{2}(3S_{yy}\varphi_y + S_{yyy}\varphi_0). \tag{7.104}$$

Introducing these relations in (7.97) we get

$$\begin{aligned}\varphi_{yy}^+ &= \varphi_{yy}^- \\ &+ \tan \theta [3(S_{yy}^-\varphi_y^- + S_{yy}^+\varphi_y^+) + (S_{yyy}^- + S_{yyy}^+)\varphi_0] \\ &+ \tan^2 \theta \frac{3}{4} [(S_{yy}^-)^2 - (S_{yy}^+)^2] \\ &+ C_2 \frac{\sin \theta}{\cos^2 \theta} (\varphi_y^- - \varphi_y^+) \\ &- \frac{C_2}{2 \cos \theta} (S_{yy}^- + S_{yy}^+) \varphi_0,\end{aligned}\tag{7.105}$$

which ends our set of bouncing rules for the amplitude coefficients up to second order.

To find the continuous time evolution of the amplitudes we can use the solution of the Hamilton-Jacobi equation to drive the differential equations (7.101) for the amplitudes. From the first equation in (7.101) and the initial condition $\varphi_0(0) = 1$ we get

$$\varphi_0(t) = \frac{Et_0^{1/2}}{(t+t_0)^{1/2}}. \tag{7.106}$$

Substituting this solution into the next equation yields

$$\varphi_y(t) = \frac{E}{(t+t_0)^{3/2}} \left[C + \frac{\frac{1}{2}At_0^{1/2}}{(t+t_0)} \right], \tag{7.107}$$

and finally after yet another substitution and a tedious calculation we get

$$\varphi_{yy}(t) = \frac{E}{(t+t_0)^{5/2}} \left[D + \frac{2AC + \frac{1}{2}Bt_0^{1/2}}{(t+t_0)} + \frac{\frac{5}{4}A^2t_0^{1/2}}{(t+t_0)^2} \right]. \quad (7.108)$$

In the last calculation we have made use of the stationarity conditions for S_{xyy} and S_{xxyy} in equation (7.101). Again the constants C, D and E are to be determined from the initial conditions of the amplitude coefficients and the previously determined constants from the phase functions. This concludes our derivation of the evolution equations for the $l = 0$ amplitude coefficients.

The general l 'th order amplitude equations for billards

Next we shall obtain the analogous amplitude evolution equations for general l 'th order eigenfunction. The l 'th order eigenfunction of course obeys the same amplitude evolution equations as the $l = 0$ eigenfunction. However, if we just start with some arbitrary function and iterate the amplitude evolution equations, we will in general end up just with the $l = 0$ eigenfunction since this is given by the leading eigenvalue of the evolution operator. This is completely analogous to iterating a matrix \mathbf{A} on a final dimensional vector \mathbf{x} . This analogy also holds for the subleading eigenfunctions: if we subtract the leading eigenvector from \mathbf{x} and iterate with \mathbf{A} we will generate the next-to-leading eigenvector etc. In our evolution operator (the amplitude equations) this subtraction of the leading eigenfunction is quite straightforward. In the semiclassical hierarchy of equations (7.51-7.52) we can simply get the $l = 1$ eigenfunction by first setting $\varphi_0^{(0)} = 0$, and then iterating. This is because of the triangular structure of the system of equations. If we keep the $\varphi_0^{(0)}$ term we cannot get anything but the $l = 0$ eigenfunction, but by removing this part we get the next eigenfunction. To get the l 'th eigenfunction one should therefore set all the coefficients $\varphi_0^{(0)}, \dots, \varphi_{l-1}^{(0)}$ equal to zero and then iterate the evolution operator on some initial wavefunction. By using these considerations we can also characterize the l 'th order eigenfunction by being the one for which all the first $l - 1$ expansion coefficients are identical zero, and which has $\varphi_l^{(0)} \neq 0$.

In two dimensions the situation is completely the same, except that we have two indeces on our expansion coefficients $\varphi_{x^n y^m}$. We also should keep in mind that all the $\varphi_{x^n y^m}$ can be obtained from pure φ_{y^m} coefficients by using the stationarity conditions (7.83). Thus it is sufficient to consider only the φ_{y^m} coefficients. The specific continuous time evolution of the amplitude coefficients of the l 'th order eigenfunction can therefore be derived from the original semiclassical equation (7.50)

$$\varphi_t + (S_x \varphi_x + S_y \varphi_y) + \frac{1}{2}(S_{xx} + S_{yy})\varphi = 0 \quad (7.109)$$

by taking the $\frac{\partial^l}{\partial y^l}$ derivative and using that we can set $\varphi_{y^k x^m} = 0$ for $k < l$. Also using the stationarity equations

$$\dot{\varphi}_{y^k x^m} = \varphi_{y^k x^{m+1}}$$

we get

$$\begin{aligned}
\dot{\varphi}_{y^l} &= -(l + \frac{1}{2}) S_{y^2} \varphi_{y^l} \\
\dot{\varphi}_{y^{l+1}} &= -(l + \frac{3}{2}) S_{y^2} \varphi_{y^{l+1}} - \frac{1}{2}(l + 1)^2 S_{y^3} \varphi_{y^l} \\
\dot{\varphi}_{y^{l+2}} &= -(l + \frac{5}{2}) S_{y^2} \varphi_{y^{l+2}} - \frac{1}{2}(l + 1)^2 S_{y^3} \varphi_{y^{l+1}} \\
&\quad - \frac{(l + 2)(l + 1)}{2} (\frac{l}{3} + \frac{1}{2}) S_{y^4} \varphi_{y^l} \\
&\quad - \frac{(l + 2)(l + 1)}{4} S_{x^2 y^2} \varphi_{y^l} \\
&\quad - \frac{(l + 2)(l + 1)}{2} S_{xy^2} \varphi_{xy^l}
\end{aligned} \tag{7.110}$$

for the semiclassical equations. The solutions to these equations are easily obtained

$$\begin{aligned}
\varphi_{y^l}(t) &= E \left(\frac{t_0}{t + t_0} \right)^{l+1/2} \\
\varphi_{y^{l+1}}(t) &= \frac{E}{(t + t_0)^{l+3/2}} \left[C + \frac{A}{2}(l + 1)^2 t_0^{l+1/2} \frac{1}{t + t_0} \right] \\
\varphi_{y^{l+2}}(t) &= \frac{E}{(t + t_0)^{l+5/2}} \left\{ D + \frac{1}{t + t_0} \left[\frac{(l + 2)^2}{2} AC \right. \right. \\
&\quad + B t_0^{l+1/2} \frac{(l + 2)(l + 1)}{2} (\frac{l}{3} + \frac{1}{2})] \\
&\quad + \frac{1}{2(t + t_0)^2} A^2 t_0^{l+1/2} \left[\frac{(l + 2)^2(l + 1)^2}{4} \right. \\
&\quad \left. \left. + \frac{3}{2}(l + 2)(l + 1)(\frac{l}{3} + \frac{1}{2}) \right] \right\}
\end{aligned} \tag{7.111}$$

Next we should derive the semiclassical bouncing equations for the amplitudes. The nonvanishing terms in φ^l are

$$\begin{aligned}
\varphi^l &= \frac{y^l}{l!} [\varphi_{y^l} + \frac{1}{l+1} \varphi_{y^{l+1}} y + \frac{1}{(l+1)(l+2)} \varphi_{y^{l+2}} y^2 \\
&\quad + \varphi_{xy^l} x + \frac{1}{2} \varphi_{x^2 y^l} x^2 + \frac{1}{l+1} \varphi_{y^{l+1} x} y x],
\end{aligned} \tag{7.112}$$

where we note the factor $\frac{y^l}{l!}$ in front of the expression. As usual we now expand the incoming and outgoing amplitude in the intermediate coordinate system and set

$$\varphi_{in} = \varphi_{out} \tag{7.113}$$

on the bouncing point on the wall. Because of the above factor $\frac{y^l}{l!}$ we can now write the bouncing condition

$$\varphi_{y^l}^+ + \frac{1}{l+1} \varphi_{y^{l+1}}^+ y_{out} + \dots = \left(\frac{y_{in}}{y_{out}} \right)^l \times [\varphi_{y^l}^- + \frac{1}{l+1} \varphi_{y^{l+1}}^- y_{in} + \dots]$$

Since to get the first correction where we only need $\varphi_2^{l(0)}$ according to second item in the recipe, we only have to compare terms up to the second order in y (on the wall). We therefore expand the fraction factor to second order in y . Using the coordinate transformations (7.86-7.87) this reads

$$\begin{aligned} \left(\frac{y_{in}}{y_{out}}\right)^l &= (-1)^l \left(\frac{1 - ay - by^2}{1 + ay + by^2}\right)^l \\ &= (-1)^l (1 - 2lay + 2l(la^2 - b)y^2 + \mathcal{O}(y^3)) \end{aligned} \quad (7.114)$$

where

$$a = \frac{C_2}{2} \tan \theta, \quad b = \frac{C_3}{6} \tan \theta$$

The detailed equations (7.114) then become

$$\begin{aligned} \varphi_{y^l}^+ + y(\varphi_{y^l x}^+ \sin \theta + \frac{\varphi_{y^{l+1}}^+}{l+1} \cos \theta) &+ \\ y^2(-\varphi_{xy^l}^+ \cos \theta \frac{C_2}{2} + \frac{\varphi_{y^{l+1}}^+}{l+1} \sin \theta \frac{C_2}{2}) &+ \\ \frac{1}{2} \sin^2 \theta \varphi_{y^l x^2}^+ + \sin \theta \cos \theta \frac{\varphi_{xy^{l+1}}^+}{l+1} &+ \\ \frac{\varphi_{y^{l+2}}^+ \cos^2 \theta}{(l+1)(l+2)} &= (-1)^l [1 - l \tan \theta C_2 y + 2l(l \frac{C_2^2 \tan^2 \theta}{4} - \frac{C_3}{6} \tan \theta) y^2] \\ &\times [\varphi_{y^l}^- + y(\varphi_{y^l x}^- \sin \theta - \frac{\varphi_{y^{l+1}}^-}{l+1} \cos \theta)] \\ &+ y^2(\varphi_{xy^l}^- \cos \theta \frac{C_2}{2} + \frac{\varphi_{y^{l+1}}^-}{l+1} \sin \theta \frac{C_2}{2}) \\ &+ \frac{1}{2} \sin^2 \theta \varphi_{y^l x^2}^- - \sin \theta \cos \theta \frac{\varphi_{xy^{l+1}}^-}{l+1} \\ &+ \frac{\varphi_{y^{l+2}}^- \cos^2 \theta}{(l+1)(l+2)}]. \end{aligned}$$

This gives the equations

$$\varphi_{y^l}^+ = (-1)^l \varphi_{y^l}^-, \quad (7.115)$$

$$\varphi_{y^{l+1}}^+ = (-1)^{l+1} (\varphi_{y^{l+1}}^- - C_2(l+1)^2 \frac{\tan \theta}{\cos \theta} \varphi_{y^l}^-), \quad (7.116)$$

to the zeroth and first order in y , and

$$\begin{aligned} \varphi_{y^{l+2}}^+ &= (-1)^l \varphi_{y^{l+2}}^- \\ &+ ((-1)^l \varphi_{xy^l}^- + \varphi_{xy^l}^+) \frac{C_2(l+1)(l+2)}{2 \cos \theta} \end{aligned}$$

$$\begin{aligned}
& + ((-1)^l \varphi_{y^{l+1}}^- - \varphi_{y^{l+1}}^+) \frac{\sin \theta C_2(l+2)}{2 \cos^2 \theta} \\
& + ((-1)^l \varphi_{y^l x^2}^- - \varphi_{y^l x^2}^+) \frac{(l+1)(l+2) \tan^2 \theta}{2} \\
& - ((-1)^l \varphi_{x y^{l+1}}^- + \varphi_{x y^{l+1}}^+) (l+2) \tan \theta \\
& - (-1)^l ((\varphi_{y^l x}^- \sin \theta - \frac{\varphi_{y^{l+1}}^-}{(l+1)} \cos \theta) \frac{l \tan \theta C_2(l+1)(l+2)}{\cos^2 \theta} \\
& + (-1)^l (\frac{l C_2^2 \tan^2 \theta}{4} - \frac{C_3 \tan \theta}{6}) \varphi_{y^l}^- \frac{2l(l+1)(l+2)}{\cos^2 \theta}, \tag{7.117}
\end{aligned}$$

to the second order in y .

The last equation can of course again be simplified by using the stationarity conditions for the mixed derivatives, which yields a formula similar to (7.105). This ends our derivation of the discontinuous evolution of the l 'th order amplitude coefficients at the bouncing points.

The first \hbar correction for billards

To get the first \hbar correction $C_l^{(1)}$ to the local eigenvalues R_l we use (7.57) and get

$$C_l^{(1)} = \frac{\varphi^{l(1)}(T_p)}{\exp(C_l^{(0)})}, \tag{7.118}$$

To get the time dependance of the full function $\varphi^{l(1)}$ we have to solve the amplitude equation to first order in \hbar and to order x^l in the one-dimensional case. Since we shall later need the result for 2-dimensional billard systems we here show how the calculation goes in this case. This also illustrates how the stationarity conditions (7.82,7.83) are applied in general. In two dimensions we therefore have to solve the amplitude equation up to order $x^m y^n$ where $m+n=l$. From the stationarity conditions (7.83) we get

$$\dot{\varphi}_{x^m y^n} = S_x \varphi_{x^{m+1} y^n} \tag{7.119}$$

which can be used to reduce all the mixed amplitude coefficients to time derivatives of pure φ_{y^n} coefficients. It is therefore sufficient to look at the equation of order y^l . Now the original amplitude equation reads

$$\partial_t \varphi + \nabla \varphi \nabla S + \frac{1}{2} \varphi \Delta S - \frac{i\hbar}{2} \Delta \varphi = 0. \tag{7.120}$$

We now should find out which ingredients are needed in this equation to get the first order in \hbar and the order y^l . Since we are dealing with the l 'th solution we can put all the amplitude coefficients $\varphi_{x^n y^m} = 0$ for $m < l$, because of the triangular structure of the hierarchy of equations. This simplifies the situation considerably. Next we can select our coordinate system so that the x-axis is

directed along the momentum direction. This means that the zeroth order of the gradient of the phase function will take the form

$$\begin{aligned}\nabla S &= \vec{p} \\ &= (1, 0),\end{aligned}\tag{7.121}$$

where \vec{p} is the momentum set to $|\vec{p}| = 1$.

Expanding the amplitude in a power series around the periodic orbit like in (??) we get the following necessary ingredients

$$\begin{aligned}\dot{\varphi}^l &= \frac{y^l}{l!} (\dot{\varphi}_{y^l} - \dot{x}_{cl} \varphi_{y^l x} + \dots) \\ \nabla \varphi^l &= (\varphi_{y^l x} y^l / l! + \dots, \varphi_{y^{l+1}} y^l / l! + \varphi_{y^l} y^{l-1} l / l! + \dots) \\ \Delta \varphi^l &= \frac{y^l}{l!} (\varphi_{y^l x^2} + \varphi_{y^{l+2}}) + \dots,\end{aligned}\tag{7.122}$$

and for the phase function we get similarly

$$\begin{aligned}\nabla S &= (S_x + S_{xy} + \dots, S_y + S_{y^2} y + \dots) \\ \Delta S &= S_{x^2} + S_{y^2} + \dots \\ &= S_{y^2} + \dots,\end{aligned}\tag{7.123}$$

where we in the last equation used that $S_{x^2} = 0$ since by the stationarity conditions this is proportional to the time derivative of S_x which is zero since S_x is the constant momentum p_x . The differential equation for the l 'th amplitude function now reads

$$\dot{\varphi}_{y^l}^{(1)} - \dot{x}_{cl} \varphi_{y^l x}^{(1)} + \varphi_{y^l x}^{(1)} S_x + S_y \varphi_{y^{l+1}}^{(1)} + l S_{y^2} \varphi_{y^l}^{(1)} = \varphi_{y^l x^2}^{(0)} + \varphi_{y^{l+2}}^{(0)}\tag{7.124}$$

to the first order in \hbar . This implies

$$\dot{\varphi}_{y^l}^{(1)} + \left(l + \frac{1}{2}\right) S_{y^2} \varphi_{y^l}^{(1)} = \varphi_{y^l x^2}^{(0)} + \varphi_{y^{l+2}}^{(0)}\tag{7.125}$$

to the zeroth order in \hbar we get analogously

$$\dot{\varphi}_{y^l}^{(0)} + \left(l + \frac{1}{2}\right) S_{y^2} \varphi_{y^l}^{(0)} = 0\tag{7.126}$$

The last equation immediately yields

$$\begin{aligned}\varphi_{y^l}^{(0)}(t) &= \exp\left(-\frac{2l+1}{2} \int_0^t S_{y^2} dt'\right) \\ &= \exp(C_l^{(0)})\end{aligned}$$

which is the two-dimensional equivalent to the result (7.60). We can therefore write the solution of equation (7.125) as

$$\varphi_{y^l}^{(1)}(t) = \exp\left(-\frac{2l+1}{2} \int_0^t S_{y^2} dt'\right) \int_0^t (\varphi_{y^l x^2}^{(0)} + \varphi_{y^{l+2}}^{(0)}) \exp\left(\frac{2l+1}{2} \int_0^t S_{y^2} dt'\right) dt'\tag{7.127}$$

and the first correction finally reads

$$C_l^{(1)} = \int_0^{T_p} \frac{(\varphi_{y'x^2}^{(0)} + \varphi_{y'^+2}^{(0)})}{\varphi_{y'}^{(0)}} dt \quad (7.128)$$

This concludes the derivation of the first order \hbar correction term in the case of two dimensional billiards. To implement this integration one should determine the phase and amplitude coefficients for each individual periodic orbit. This we shall do in section (7.7).

7.7.1 A numerical algorithm to calculate the first \hbar correction

The above derivations now allow us to follow an initial wave along the periodic orbit. Each such iteration changes the initial amplitude coefficients and will for almost all initial conditions converge to the leading eigenfunction of the evolution operator. To get the action coefficients and the leading amplitude function we can therefore just select a set of initial S and φ coefficients and iterate the evolution equations derived above while properly normalizing the amplitudes after each iteration.

Now the iteration sequence goes as follows: choose initial (random) values of the derivative constants of the action function. From these you calculate the initial values of t_0 , A and B :

$$\begin{aligned} t_0 &= 1/S_{yy}(0) \\ A &= S_{yyy}(0)t_0^3 \\ B &= S_{yyyy}(0)t_0^4 + 3t_0 - \frac{3A^2}{t_0} \end{aligned}$$

Then you evolve the S_{y^n} 's to the first bouncing point is reached. Here one makes use of the derived bouncing relations to establish the $S_{y^n}(t_i^+)$ values. These are then used to calculate the new constants t_0 , A and B . In this way one can by a few iterations around the periodic orbit obtain the action function corresponding to the local Schrödinger problem. Actually the calculation can be speeded up a bit since we can calculate the S_{yy} term directly from the solution of the rational fraction transformation of the curvature matrix \mathbf{M} which were derived in section 5.3.1. In the two dimensional case this can be demonstrated very easily: First we have to find the Jacobian of the periodic orbit which we also need to in the case of the usual Gutzwiller-Voros zeta function. To find \mathbf{M} we need in general to work on the symplectic matrix \mathbf{T} that diagonalizes \mathbf{J} . We know that \mathbf{T}^{-1} must contain the eigenvectors of \mathbf{J} so that we can write

$$\mathbf{T}^{-1} = \begin{bmatrix} u_1 & s_1 \\ u_2 & s_2 \end{bmatrix} \quad (7.129)$$

where \mathbf{u} is the unstable and \mathbf{s} is the stable eigenvector. Then \mathbf{T} is given by

$$\mathbf{T} = \frac{1}{\det \mathbf{T}^{-1}} \begin{bmatrix} s_2 & -s_1 \\ -u_2 & u_1 \end{bmatrix} \quad (7.130)$$

and from the solution formula (5.62) for \mathbf{M} we obtain

$$\begin{aligned}\mathbf{M} &= -\mathbf{T}_{pp}\mathbf{T}_{pq}^{-1} \\ &= u_2/u_1 \quad \text{or} \quad s_2/s_1\end{aligned}\tag{7.131}$$

where the last solution corresponds to interchanging the rows of \mathbf{T} . Here in the two dimensional case the \mathbf{M} solutions are then just the slopes of the invariant manifolds at the periodic orbit (see fig. refmanifolds in appendix 9.1). To get an explicit expression for \mathbf{M} (which in this case is actually just the Sinai Bunimovic curvature κ) in terms of the ingredients of the Jacobian and the stability, we note that the eigendirections can also be represented in the form

$$\begin{aligned}\tilde{\mathbf{u}} &= \begin{bmatrix} 1 \\ \kappa_u \end{bmatrix} \\ \tilde{\mathbf{s}} &= \begin{bmatrix} 1 \\ \kappa_s \end{bmatrix}\end{aligned}$$

and we then have

$$\mathbf{J}\tilde{\mathbf{u}} = \Lambda\tilde{\mathbf{u}}$$

which then gives

$$\kappa_u = (\Lambda - J_{11})/J_{12}\tag{7.132}$$

and similarly for the stable direction. For the ‘0’ orbit of the $R : a = 6.0$ 3-disk system the exact calculation yields $\kappa_u = 2.224744871\dots$, whereas the numerical algorithm sketched above gives $\kappa_u = 2.224744871\dots$ after 25 iterations. This is of course the same result (7.38) as we obtained in section (7.3) by iterating the rational fraction transformation for the Sinai Bunimovic curvature. In higher dimensions the \mathbf{M} solution formula (5.62) of course provides this first step as well.

The evolution of the amplitudes take place in exactly the same fashion. The equations for the constants are here:

$$\begin{aligned}E &= a(0) \equiv 1 \\ C &= \frac{t_0^{3/2}}{E} \varphi_y(0) - \frac{A}{2t^{1/2}} \\ D &= \frac{t_0^{5/2}}{E} \varphi_{yy}(0) - \frac{2AC + \frac{Bt_0^{1/2}}{2}}{t_0} - \frac{5A^2}{4t_0^{3/2}}\end{aligned}\tag{7.133}$$

where the $a(0)$ constant is fixed by normalization after each iteration.

When these calculations are done we have just to calculate the correction $C_l^{(1)}$ by means of the integral (7.128). A program that performs this calculation is listed in appendix 9.3.

Putting the results of the constants t_0, A, B, C, D and E into the expression (7.128) for the first order \hbar correction we get

$$\begin{aligned}
C_l^{(1)} &= \int_0^{T_p} \frac{\varphi_{y^{l+2}} + \varphi_{y^l x^2}}{\varphi_{y^l}} dt \\
&= \int_0^{T_p} dt \frac{1}{(t+t_0)^2} \left[\frac{D}{t_0^{l+1/2}} + (l+\frac{1}{2})(l+\frac{3}{2}) \right] \\
&+ \frac{1}{(t+t_0)^3} \left[\frac{(l+2)^2}{2} \frac{AC}{t_0^{(l+1/2)}} + B \frac{(l+1)(l+2)}{2} \left(\frac{l}{3} + \frac{1}{2} \right) \right] \\
&+ \frac{1}{(t+t_0)^4} \frac{A^2}{2} \left\{ \frac{(l+1)^2(l+2)^2}{4} + \frac{(l+1)(l+2)}{2} \left(\frac{l}{3} + \frac{1}{2} \right)^3 \right\}
\end{aligned} \tag{7.134}$$

which finally gives

$$\begin{aligned}
C_l^{(1)} &= \left[(l+\frac{1}{2})(l+\frac{3}{2}) + \frac{D}{t_0^{(l+1/2)}} \right] \frac{t}{t_0(t+t_0)} \\
&+ \left[(l+2)^2 \left(\frac{AC}{4} \right) / \left(t_0(l+\frac{1}{2}) \right) + (l+2)(l+1)(l+\frac{3}{2})B/12 \right] \\
&\times \frac{t(t+2t_0)}{(t_0(t+t_0))^2} \\
&+ (l+1)(l+2) \left[(l^2+3l+2)\frac{1}{2} + l + \frac{3}{2} \right] \frac{A^2}{12} \\
&\times \left(\frac{1}{t_0^3} - \frac{1}{(t+t_0)^3} \right)
\end{aligned} \tag{7.135}$$

7.8 Application to the 3-disk system

To test our method outlined above we here investigate how it works on the three disk scattering system. Taking as starting point the \hbar corrected spectral determinant (7.68)

$$\Delta(E) = \prod_l \zeta_l^{-1}(E) \tag{7.136}$$

we can study either the entire determinant or the individual quantum zetafunctions

$$\zeta_l^{-1}(E) = \prod_p \left(1 - \exp(iS_p(E)/\hbar) + \sum_m (i\hbar/2)^m C_l^{p(m)}(E) \right). \tag{7.137}$$

where we can get the leading resonances from the $l = 0$ zeta function.

For the 3-disk system our calculation involved the 226 shortest periodic orbits of the system including all cycles up to topological length 10. We computed the corrections to these orbits in the fundamental domain, since our method

makes it possible to utilize the symmetry reduction of Cvitanović and Eckhardt [16]. The results can be compared to the exact quantum resonances as well as to the pure semiclassical calculation based on the usual Gutzwiller Voros determinant. We have studied the leading scattering resonances in the region $0 \leq \text{Re}k \leq 200$ and $-0.5 \leq \text{Im}k \leq 0$, in the complex k -plane, by using the Gutzwiller-Voros zeta function and also by just using the leading quantum zeta function $\zeta^{-1}(k)$ with and without the \hbar corrections. The latter has been done for comparison reasons with Ref. [33].

We start by considering the shortest periodic orbit in the 3-disk system, which is the one bouncing back and forth between the same two disks. The situation is here similar to that in the confocal hyperbola problem, where the first correction term to the Gutzwiller trace formula has been computed numerically [59]. The geometry of the orbit in these problems is so simple that we can calculate the first correction term directly. The result of this calculation yields

$$C_0^{0(1)} = \frac{1}{p} \left(C_2 - \frac{3}{8} C_2 \frac{2 + LC_4/3C_2^2}{2 + C_2 L} \right), \quad (7.138)$$

where C_2 and C_4 denotes the expansion coefficients of the wall at the bouncing point and where L is the length of the periodic orbit. This result can be compared with the findings of ref.[33] for the two disk system and with those of ref.[59] for the confocal hyperbolae. In case of the two disk scattering system $C_2 = 1/a$ and $C_4 = 3/a^3$, where a is the radius of the disk. In this case we get

$$C_0^{(1)} = \frac{5}{8ap}, \quad (7.139)$$

which coincides with the result of Ref.[33] derived via Feynman graph technique. In the case of the two disc scattering system our results will therefore be identical to the results of Ref [33]. In the case of the confocal hyperbolae we have $C_4 = -6C_2^2/L$, and the correction is

$$C_0^{(1)} = \frac{C_2}{p}, \quad (7.140)$$

which was numerically confirmed in ref.[59].

Next we study the \hbar corrections to the genuine 3-disk orbits. First we can try to compare our \hbar corrections $C_0^{(1)}$ to the fullspace calculation of Ref [33]. Here we do not use the symmetry reduction, but find the first correction to all the 25 shortest orbits of topological length up to 9 in the full 3-disk domain. The calculation can then be compared directly with the results in [33]. Our results are listed in table (7.1). We see that the two calculations which takes quite different approaches gives the same results except for a few of the orbits. On the base of the results in table 7.1 Gaspard et al. also calculates the first few resonances of the 3-disk system using the full space dynamical

Orbit	deg.	$C_{0,GA}^{(1)}$	$C_{0,VR}^{(1)}$
12	3	0.62500	0.62500
123	2	1.68647	1.68647
1213	3	2.03980	2.03979
12123	6	2.45127	2.45127
121323	3	3.11233	3.11383
121213	6	2.68951	2.68951
1212123	6	3.07848	3.07846
1212313	6	3.24027	3.24026
1213123	6	3.74224	3.70424
12121213	6	3.31483	3.31483
12121313	3	3.34018	3.34017
12121323	6	3.75662	3.75662
12123123	6	4.13736	4.13736
12123213	6	3.93185	3.93185
12132123	3	4.24438	4.24438
121212123	6	3.70350	3.70349
121212313	6	3.86777	3.86776
121212323	6	3.86777	3.86776
121213123	6	4.35071	4.35071
121213213	6	4.35071	4.35071
121231323	6	4.46254	4.46254
121231213	6	4.49403	4.49403
121232123	6	4.49403	4.49403
121232313	2	4.06479	4.06478
121321323	6	4.80313	4.80312

Table 7.1: The first order \hbar correction for the first 25 orbits in the full 3-disk scattering system. First two columns show the symbolic representation of the periodic orbit and its symmetry degeneracy. Next two columns show the \hbar correction obtained by Gaspard and Alonso, and the \hbar correction obtained by our method, respectively.

quantum zeta function and periodic orbits up to topological length 8 and 9. We tried to compare the analogue fundamental domain calculation to these results using only the first five periodic orbits (all up to topological length 3) in the fundamental domain as input in the dynamical $l = 0$ quantum zeta function. The results are displayed in figure 7.2 together with the resonances from [33].

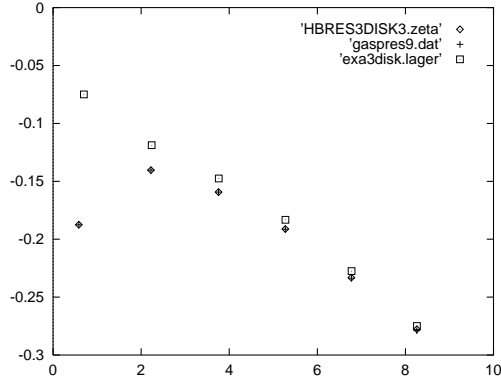


Figure 7.2: The first 6 A_1 resonances in the $R : a = 6.0$ 3-disk scattering system. The squares denotes the exact data from A. Wirzba, crosses denotes the full space calculation to curvature order 9 of Gaspard and Alonso and finally diamonds denotes our fundamental domain calculation using the shortest 5 periodic orbits as input. The last two calculations are both corrected to the first order in \hbar .

Next we can compare our results for the leading A_1 resonances to the exact data which are provided by A. Wirzba. First we note that at curvature order 7 the \hbar corrected as well as the usual Gutzwiller-Voros zeta function resonances does not change in the leading digits by inclusion of more periodic orbits, and that they are located basically on top of the exact resonances. In the following calculations we therefore keep the truncation of the cycle expansions at topological order 7. The leading part of the resonance spectrum is depicted in figure 7.3 As it can be seen it is not difficult to identify the exact resonances with the corresponding semiclassical Gutzwiller-Voros and \hbar corrected resonances. From this correspondance we can compare the pure semiclassical results to the \hbar corrected calculation. We do this by plotting the deviation in real and imaginary k from the corresponding exact resonance as a function of for instance $\text{Re}k$. A plot like this is shown in figure 7.4 The \hbar corrected resonances are seen to be clearly better than the ordinary Gutzwiller-Voros resonances. Even more instructive it might be to look at a plot of the relative error of the resonances, that is the ratio $|\text{Re}k_{\hbar} - \text{Re}k_{\text{exact}}| / |\text{Re}k_{GV} - \text{Re}k_{\text{exact}}|$ as function of $\text{Re}k$ or $\text{Im}k$ and the analogous plots for the imaginary part. Such two plots are shown in figures 7.6 and 7.7 By comparing the two figures one can see that in general the \hbar corrected resonances are much better than the semiclassical resonances except for a very few resonances in the area $\text{Re}k \geq 100$ and for $\text{Im}k \leq -0.4$. For instance the 8 resonances where the relative deviation is larger than or of order 1, are all located far down in the complex plane. By inclusion of the $l = 1$

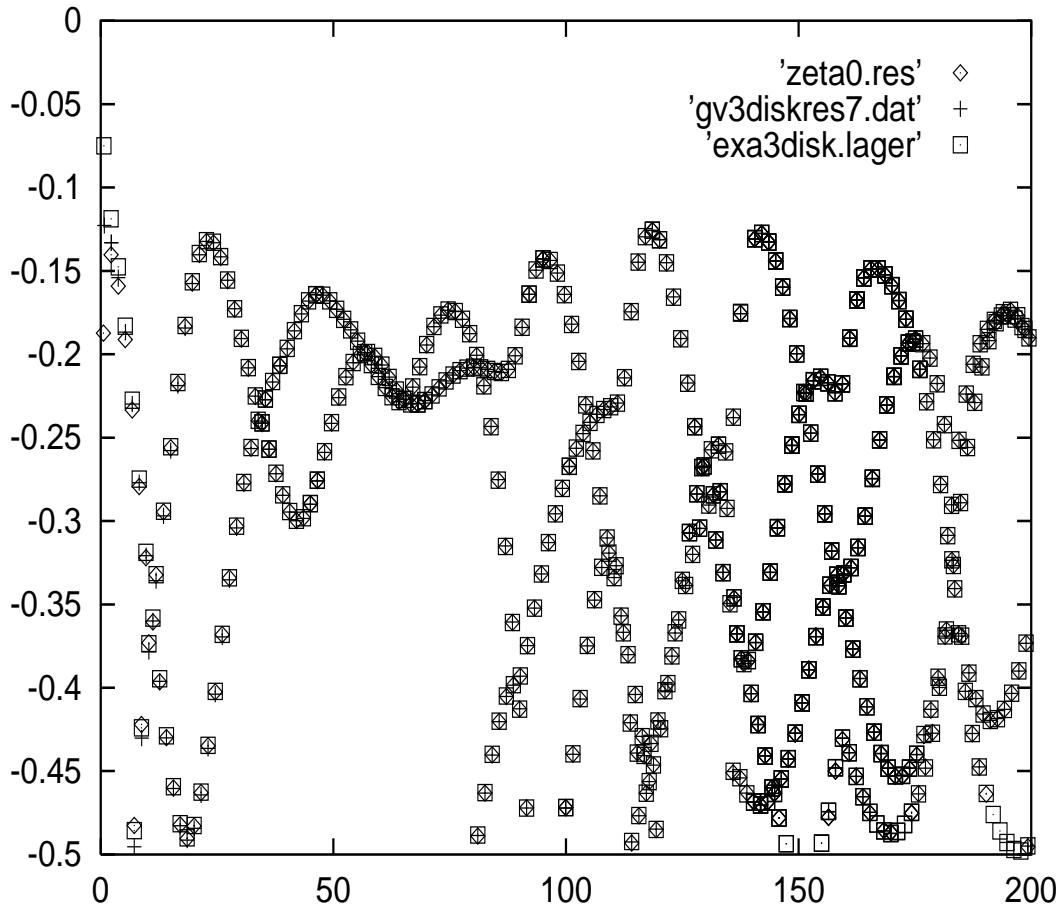


Figure 7.3: The leading part of the A_1 resonance spectrum of the $R : a = 6.0$ 3-disk scattering system. The exact spectrum is from A. Wirzba and is denoted with dotted squares. The Gutzwiller-Voros zeta function resonances are denoted with a '+' and the \hbar corrected resonances from the $l = 0$ quantum zeta function with a \diamond .

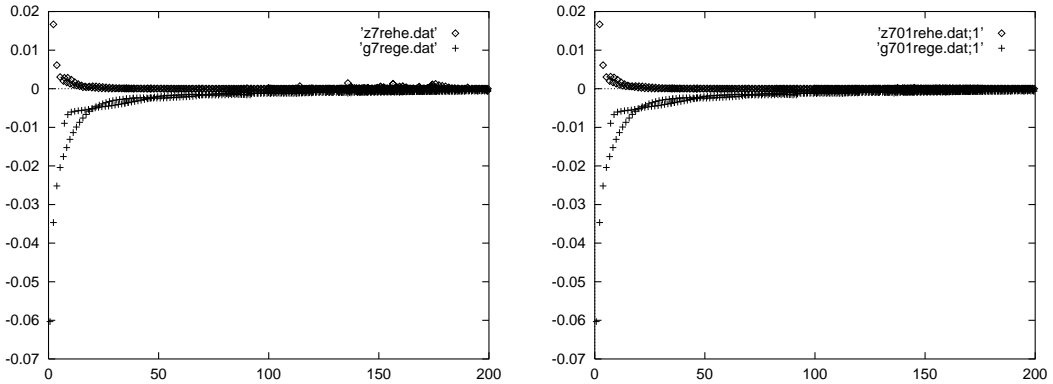


Figure 7.4: The deviation in real part of the Gutzwiller Voros resonances and the \hbar corrected $l = 0$ and $l = 1$ quantum zeta resonances (\diamond) from the exact quantum resonances. The exact data are from A. Wirzba. By inclusion of $l = 2, 3$ the picture does not change in a visible way.

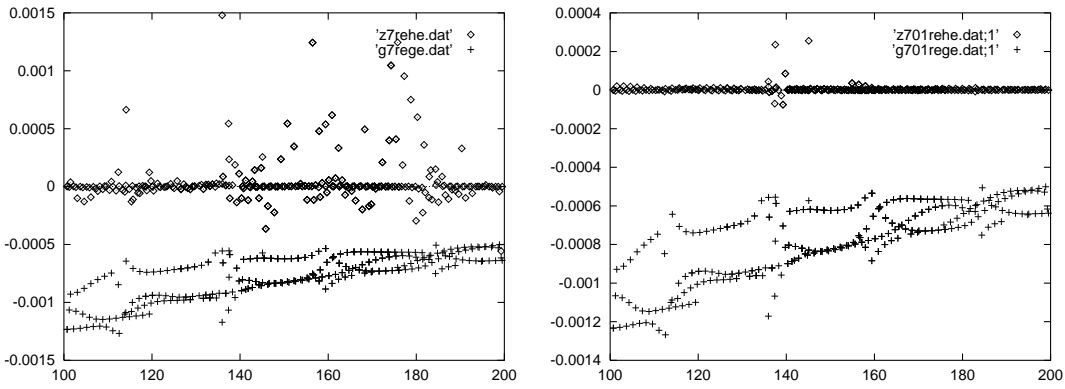


Figure 7.5: The same as above except the different $\text{Re } k$ domain.

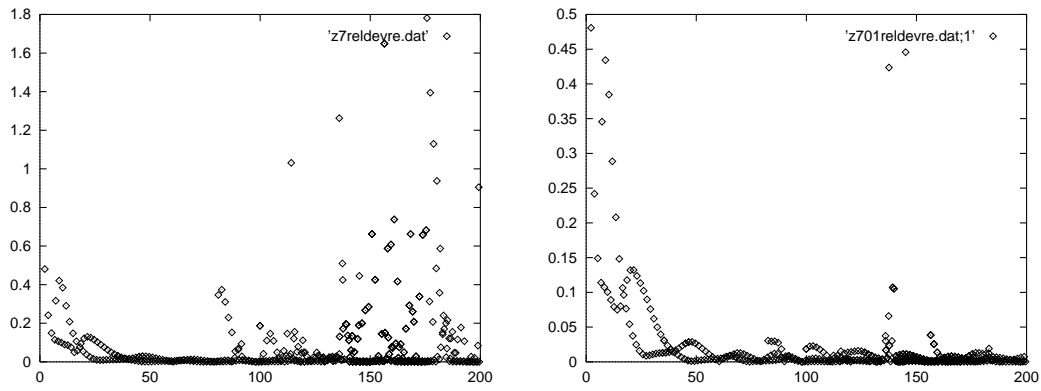


Figure 7.6: Relative deviation in real part of k as function of $\text{Re } k$. The first picture compares the Gutzwiller-Voros zeta function resonances to the $l = 0$ dynamical quantum zeta resonances with the first \hbar correction included. In the right side picture both $l = 0, 1$ are included with the first \hbar correction. Note the different scales on the y -axis.

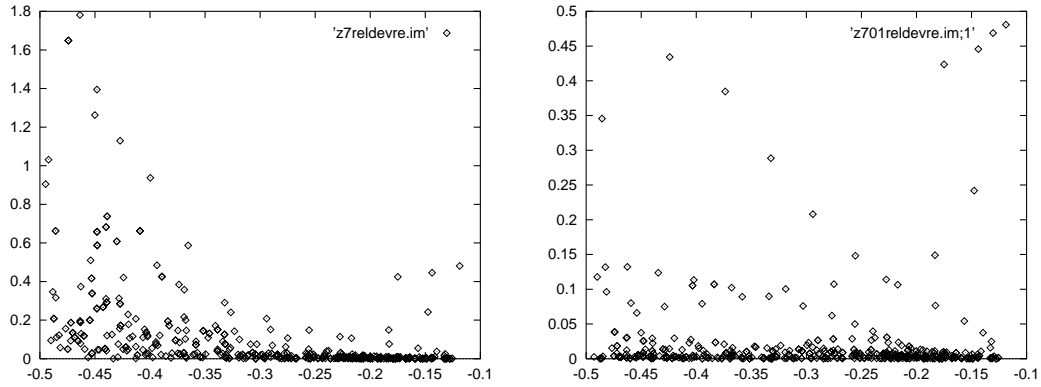


Figure 7.7: Relative deviation in real part of k as function of $\text{Im } k$. The same calculations as in the previous figure are compared. Again one should note the different scales in the y -axis.

corrected quantum zeta function as well the picture improves further: whereas for the first quantum zeta most of the resonances improved by a factor 2 in real part of k , we obtain by inclusion of the next corrected zeta function an improvement of a factor 20 for most of the resonances. By inclusion of further zeta functions this picture does not change considerably at least not by inclusion of the first four $l = 0, 1, 2, 3$ quantum zeta functions.

The leading part of the A_1 resonance spectrum is therefore in general improved by a factor 2-20, in the real part of k , by inclusion of the first \hbar correction in the first few zeta functions of the Gutzwiller-Voros product.

Making the analogue plots for the deviation in imaginary part results in figures 7.8 and 7.10. Here we see basically the same tendency as for the real

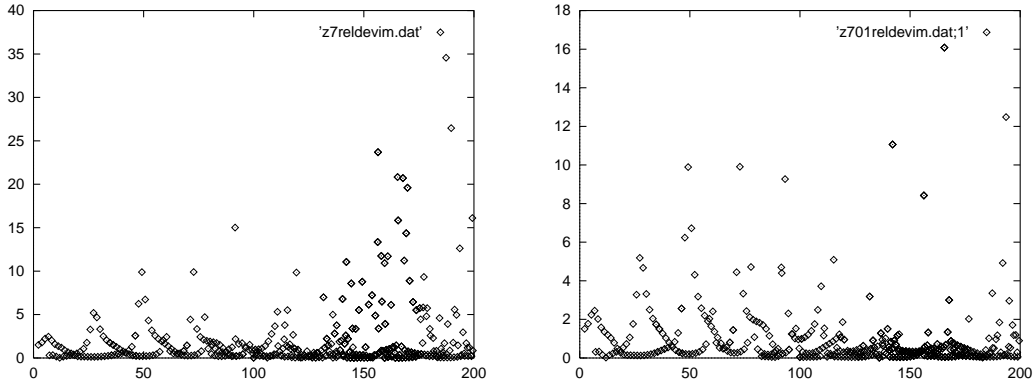


Figure 7.8: Relative deviation in imaginary part of k as function of $\text{Re}k$. The first picture compares the Gutzwiller-Voros zeta function resonances to the $l = 0$ dynamical quantum zeta resonances with the first \hbar correction included. In the right side picture both $l = 0, 1$ are included with the first \hbar correction. Note the different scales on the y -axis.

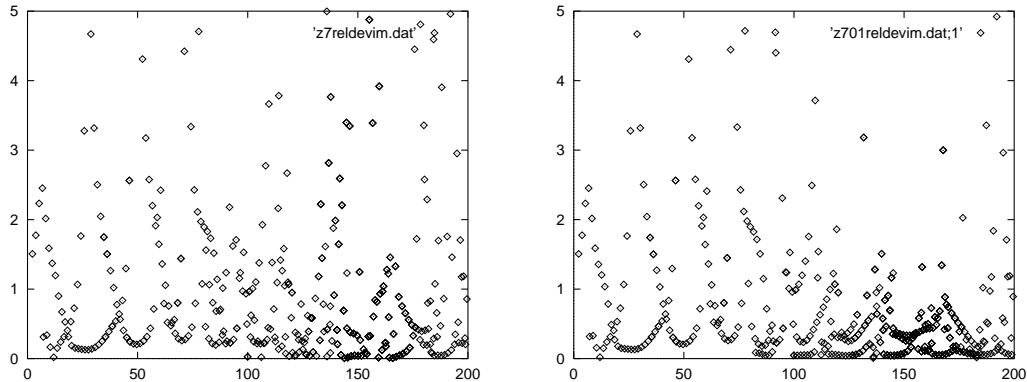


Figure 7.9: A blow-up of the previous picture reveals that approximately only half of the resonances are improved in the imaginary part.

part except that approximately only half of the resonances are improved in imaginary part by the inclusion of the \hbar correction. The picture is thus not

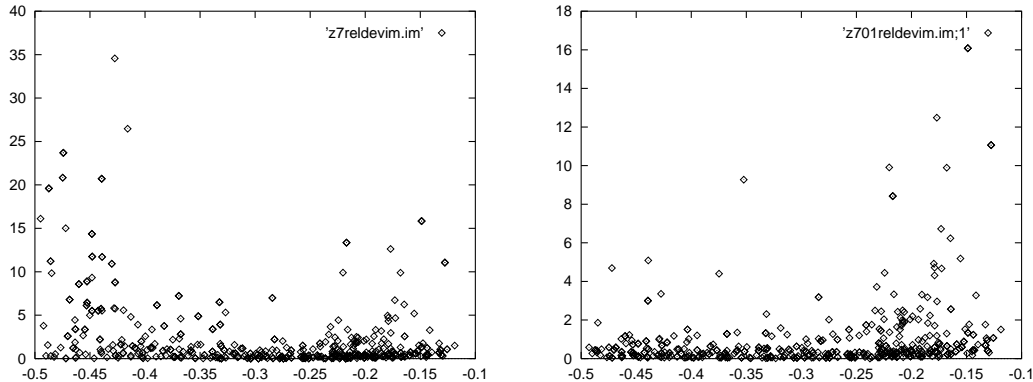


Figure 7.10: Relative deviation in imaginary part of k as function of $\text{Im}k$.

as clear as for the real part: most of the \hbar corrected resonances are as good as, or even better than their semiclassical counterparts but for some resonances the situation is completely opposite. The reason for this is at least partially explained by Gaspard who observed that the *first order* \hbar correction entering in the Gutzwiller-Voros zeta function has the same phase as the stability whereas the second order \hbar correction has an additional $e^{i\pi/2}$ phase. Consequently the first order \hbar correction improves the real part of the resonance whereas we have to go to second order in the \hbar expansion to also improve the imaginary part of the resonances. So even though we also observe an improvement for half of the resonances by inclusion of only the first order \hbar correction, the above explanation might account for the other resonances. This could of course be investigated by using the procedure outlined in this section to obtain also the second order \hbar correction to the local eigenvalues. However, also in the case of the imaginary deviation we see a considerable improvement when going from the pure \hbar corrected quantum zeta function to the product of the first few \hbar corrected zeta functions. This can clearly be seen from the figures 7.8 and 7.10 by noting the different scale on the y -axis.

Generally we note, that the relative error of the corrected calculation versus the error of the semiclassical calculation decreases with the real part of the wavenumber and increases with the magnitude of the imaginary part of the wavenumber. By inclusion of still more corrected zeta functions in the Gutzwiller-Voros product we at first see a nice improvement. We do not expect this to continue when including still further corrected zeta functions in the product. This is because the \hbar expansion is only an asymptotic series: From (7.135) we see that the first order correction $C_l^{(1)}$ is at most a fourth order polynomial in l . This can easily be checked by computing $C_l^{(1)}$ for $l = 1, 2, 3, \dots, l_{\max}$ and fit the result by a polynomial. For the $\overline{0}$ orbit of the 3-disk system such a fit (by Mathematica) for $l = 1, 2, \dots, 10$, yields

$$C_l^{\overline{0}(1)} = 0.625 + 1.4375l - 0.3125l^2 - 0.625l^3 - 3.32179 \times 10^{-13}l^4$$

which has been numerically confirmed by A. Wirzba in [?]. For the $\overline{1}$ orbit a

similar calculation yields

$$\begin{aligned} C_l^{\bar{1}(1)} &= 1.68647 + 3.90756l + 0.593969l^2 - 0.728335l^3 + 0.0327606l^4 \\ &\quad + 3.97459842815806 \times 10^{-14}l^5 \end{aligned}$$

For large l the numerical value of $C_l^{(1)}$ therefore diverges and the first order corrected Gutzwiller-Voros product will therefore also diverge.

7.9 Conclusions

In this chapter we have described a new method developed by G. Vattay to evaluate corrections to the leading saddle point approximation of the Feynman path integral [55]. The method reduces the problem to a set of ordinary differential equations which have to be solved at certain boundary conditions. In all orders the product structure of the functional determinant $\Delta(E)$ is maintained. One can introduce the quantum zeta functions. The corrections to the leading zeta function is easier to calculate than a general $l > 0$ term and it is very practical to use it for extended computations. Taking the theory as a starting point we found analytically the necessary ingredients for calculating the first \hbar correction term in the case of a general 2-dimensional billiard system. We obtained this formalism for a general l value, in order to be able to correct several of the quantum zeta functions $\zeta_l^{-1}(k)$. A simple numerical calculation scheme for the method has been evolved for the special case of two dimensional billiard systems. The calculation scheme which works for general values of l , was implemented in a FORTRAN program. The program only uses simple geometrical information from the periodic orbits namely the lengths of their flight sections, their transverse stabilities and the local derivatives of the walls at the bouncing points. The program is therefore immediately applicable to any two-dimensional billiard system. The program has been tested on the 3-disk scattering system and the results compared to the exact as well as the pure semiclassical calculations. The comparison shows a clear improvement in real part of k of the predicted resonances by including the first correction term. By inclusion of further corrected quantum zeta functions in the Gutzwiller-Voros product the calculation improves considerably for both the real and imaginary part of the resonances. The imaginary part of our estimates however, does not improve as dramatically as the real parts, and only approximately half of the resonances are directly improved in the imaginary part by inclusion of the first \hbar correction. We expect that inclusion of the second order \hbar correction will result in a general improvement of the imaginary part of the resonances as well.

Chapter 8

Perspectives

In this thesis we have addressed three main points concerning the general purpose of improving the semiclassical rules of quantization in hyperbolic Hamiltonian systems that classically display chaos.

First we investigated the quasiclassical propagator introduced by Vattay [53] and derived the spectral determinant for this in the general N dimensional case. As a byproduct of this we obtained an explicit solution formula to the Hamilton-Jacobi equation to the second order in the case of a periodic orbit by solving the fixpoint equation of the generalized rational fraction transformation that governs the evolution of the second derivative or curvature matrix of the phase function. By numerical calculation we showed that the determinant indeed seems to be an entire function since the expansion coefficients in the cycle expansion of the determinant exhibits a super exponential decay towards 0, indicating that the determinant has no poles. By considering the numerical studies of A. Wirzba, which are based on the periodic orbits obtained by our numerical routines, we concluded that to obtain the lowlying resonances of the $R : a = 6.0$ 3-disk system one has to expand the determinant to 12'th order in the cycle expansion. This means that one here has to do more work than is necessary when using the Gutzwiller-Voros spectral determinant. The advantage on the other hand, is that in contrast to the Gutzwiller-Voros spectral determinant the Vattay determinant is not just an asymptotic series. The resonances thus obtained will therefore stay put by inclusion of still more periodic orbits. The price we have to pay for this is then the work of obtaining more periodic orbits and to calculate the stabilities of the periodic solutions of the curvature matrix flow.

Second we introduced the geometrical theory of diffraction developed by Keller, and showed how the semiclassical expression of the propagator can be considerably improved by introducing generalized minimal action rays or creeping orbits that has no physical classical limit but still fulfills the generalized Fermat principle. In this theory the semiclassical propagator is then extended from the usual Van Vleck propagator to also include a summation over diffractive or creeping orbits that connects q with q' in time t . As a fur-

ther development of the Keller procedure we showed how diffraction from edges can also be described by this theory. By making the usual cycle expansion of a generalized spectral determinant that allows diffractive periodic orbits, and by comparing this to the exact quantum mechanical cumulant expansion for the simple 2-disk scattering system, we obtained a rule relating the ingredients of the diffractive propagator to the cycle expansion of the diffraction spectral determinant. By analyzing the order of approximation, we could derive an expression for the trace of the k domain Greens function in the case of diffractive periodic orbits by using the relation

$$\text{Tr}G(k) = -\frac{d}{dk} \ln \Delta(k). \quad (8.1)$$

By numerical investigation of the scattering resonances of our 2- and 3-disk systems and by comparison to the exact results, we showed that the semiclassical calculation including diffraction effects deviated clearly from the usual Gutzwiller-Voros results and that the correct quantum results were at least qualitatively obtained. For instance families of resonances that were not at all present in the pure geometrical calculation could be uniquely identified by resonances resulting from the diffractive spectral determinant. These new resonances however, showed a systematical deviation from the exact results. We expect that this is due to the cutoff in the Airy corrections since the numerical studies by A. Wirzba indicates a tremendous improvement of the resonances when including the higher order Airy corrections in the simple case of the 1-disk scatterer.

Our expression of the semiclassical creeping propagator still has short comings, which are open to improvements:

- The creeping expression for $G(x, x', t)$ is only valid if x' does not lie in the penumbra region i.e. x' should either be in the illuminated region or in the shadow region. So our propagator can not deal with the socalled penumbra correction introduced recently by Smilansky et al. as it stands.
- In the cycle expansion of the diffraction spectral determinant the exact cancellation of the curvature terms is only correct for the $l = 1$ modes. For higher modes one has to keep track of the full set of curvature terms, since the propagator is only multiplicative for the $l = 1$ mode.
- In the diffractive part of the propagator we make use of the Airy approximation of the Hankel function and their zeros. By numerical studies A. Wirzba [63] showed that the results of the calculations using our propagator highly improves when taking the polynomial corrections to this approximation into account. At this point however, there does not seem to be any simple way to include these corrections into the expression of the propagator and at the same time keep the nice multiplicative structure even for the $l = 1$ mode.

Third we introduced the method of obtaining \hbar corrections to the Gutzwiller trace formula by using ordinary differential equations as developed by Vattay

et. al. in [55]. Taking this theory as the *starting point* we showed how it could be specialized to the case of two dimensional billiard systems and we developed a simple algorithm that gives the contribution associated with each periodic orbit, to the first order \hbar correction to the dynamical quantum zeta functions $\zeta_l^{-1}(k)$. By applying our solution to the Hamilton-Jacobi equation obtained in the section on entire spectral determinants, we could slightly speed up this calculation. The method however, works nicely even without this result.

By calculating numerically the \hbar corrections to all the periodic orbits with topological length less than 9 in the full 3-disk system, we showed that our results are almost equivalent to the \hbar corrections obtained by Gaspar and Alonso, using the Gaussian corrections to the saddlepoint approximation. At this point it is still not clear where the origin of the small deviations in this comparison lies. In the special case of the 2-disk system the agreement is exact though.

As a further study, we calculated the first \hbar correction to the $l = 0, 1, 2, 3$ quantum zeta functions in the A_1 representation, for all the orbits up to topological length 10 in the fundamental domain of the $R : a = 6.0$ 3-disk system. The resonances of the corrected quantum zeta functions were compared to the pure semiclassical and the exact quantum resonances by including more and more corrected zeta functions in the Gutzwiller-Voros product. Generally we observed that the relative error of the corrected calculation versus the error of the semiclassical calculation decreases with the real part of the wavenumber and increases with the magnitude of the imaginary part of the wavenumber. By comparing first the $l = 0$ and next the $l = 0, 1$ product of corrected quantum zeta functions to the Gutzwiller-Voros determinant we found a good improvement of almost all the resonances of approximately a factor 2 respectively 20 in the real part of the wave number. By inclusion of further corrected quantum zeta functions in the Gutzwiller-Voros product the calculation did not improve dramatically. The imaginary part of our estimates however, does not improve as much as the real parts, and only approximately half of the resonances are directly improved in the imaginary part by inclusion of the first \hbar correction. We expect that inclusion of the second order \hbar correction will result in a general improvement of the imaginary part of the resonances as well.